Journal of Scientific Computing
https://doi.org/10.1007/s10915-018-0796-5

A Divergence Free Weak Virtual Element Method for the Stokes Problem on Polytopal Meshes

Long Chen[1,2] · **Feng Wang**[3]

Received: 11 September 2017 / Revised: 15 July 2018 / Accepted: 27 July 2018

Abstract
Some virtual element methods on polytopal meshes for the Stokes problem are proposed and analyzed. The pressure is approximated by discontinuous polynomials, while the velocity is discretized by H(div) virtual elements enriched with some tangential polynomials on the element boundaries. A weak symmetric gradient of the velocity is computed using the corresponding degree of freedoms. The main feature of the method is that it exactly preserves the divergence free constraint, and therefore the error estimates for the velocity does not explicitly depend on the pressure.

Keywords Stokes equations · Virtual element methods · H(div) element · Divergence free

1 Introduction

Let $\Omega \subset \mathbb{R}^d, d = 2, 3$ be a bounded and simply connected polytopal domain. Given an external force field $\boldsymbol{f} \in \boldsymbol{L}^2(\Omega)$, we consider the steady-state incompressible Stokes problem:

$$\begin{cases} -\operatorname{div}(2\nu\epsilon(\boldsymbol{u})) + \nabla p = \boldsymbol{f} \text{ in } \Omega, \\ \operatorname{div} \boldsymbol{u} = 0 \text{ in } \Omega, \\ \boldsymbol{u} = \boldsymbol{0} \text{ on } \partial\Omega, \end{cases} \tag{1}$$

Long Chen was supported by the National Science Foundation (NSF) DMS-1418934 and in part by the Sea Poly Project of Beijing Overseas Talents, and Feng Wang was supported by National Natural Science Foundation of China (Grant Nos. 11371199, 11371198, 11301275) and the Fund of Overseas Research and Training Program for Excellent Young and Middle-aged Teachers and Presidents in Universities and Colleges of Jiangsu.

✉ Feng Wang
fengwang@live.cn

Long Chen
chenlong@math.uci.edu

[1] Beijing Institute for Scientific and Engineering Computing, Beijing University of Technology, Beijing 100124, China

[2] Department of Mathematics, University of California at Irvine, Irvine, CA 92697, USA

[3] Jiangsu Key Laboratory for NSLSCS, School of Mathematical Sciences, Nanjing Normal University, Nanjing 210023, China

Published online: 02 August 2018

where $\epsilon(\boldsymbol{u}) = (\nabla \boldsymbol{u} + \nabla \boldsymbol{u}^{\intercal})/2$ is the symmetric gradient of $\boldsymbol{u}$, $\nu > \nu_0 > 0$ stands for the constant viscosity, $\boldsymbol{u}$ denotes the velocity field, and p is the pressure. This model describes many natural phenomena, such as the ocean currents, water flow in a pipe, and air flow around a wing etc.

There are tremendous amount of work on the numerical methods for Eq. (1), see the monographs [8,28,32] and the references therein. Traditionally, the main difficulty in proposing suitable schemes is to make the velocity space and the pressure space well coupled, i.e., satisfying the inf-sup condition, to ensure the existence and the stability of the solution. Recently, it is emphasized that (see the review paper [31]), on the discrete level, one should preserve the exact mass conservation property, i.e., the exact divergence free constraint. This is a key point to obtain a pressure-robust method.

Several divergence free elements have been proposed for two dimensional problems, see, e.g., [27,40]. It is, however, quite difficult to construct simple exact divergence free conforming elements in $\boldsymbol{H}^1$ space, especially in three dimensions. For example, Zhang [50] proved that the element $\boldsymbol{P}_k^c - P_{k-1}^{dc} (k \geq 6)$ was stable on uniform tetrahedral grids. A relatively simple divergence free finite element can be starting from the $\boldsymbol{H}(\mathrm{div})$ conforming elements, and then using some techniques to deal with the $\boldsymbol{H}^1$ requirement for the velocity. One way is adding divergence free functions, e.g., **curl** of particular bubble functions, to $\boldsymbol{H}(\mathrm{div})$ element spaces to enforce the tangential continuity and obtain a H^1-conforming or nonconforming methods, see, e.g., [30,36,49] for 2D and [29,49] for 3D. The other one is using appropriate discrete variational forms. Cockburn et al. [19] and Wang and Ye [46] introduced tangential penalty and obtained discontinuous Galerkin divergence free methods respectively, see also in [23] for the problems with more general boundary conditions. In [21], the authors proposed a class of $\boldsymbol{H}(\mathrm{div})$ conforming HDG methods based on the gradient–velocity formulation by sending the normal stabilization function to infinity in the HDG methods, see also [20,22] for the overview of other versions of HDG methods for Stokes equations. Recently by rewriting the vector Laplacian to the "curl-div" formulation and introducing a discrete dual curl operator, Chen et al. [17] proposed a divergence free MAC scheme on triangular grids. We should mention that, via the Stokes complex, some $\boldsymbol{H}^1$ divergence free finite elements were introduced from H^2 conforming elements, see, e.g., [27,29]. One can also get pressure independent error estimates by divergence preserving velocity reconstruction for some traditional finite element pairs, see, e.g., [25,33].

In the last few years, due to the great flexibility for problems on complicated geometry, numerical methods on polytopal meshes have drawn increasingly attentions. Several methods have been proposed, such as, mimetic finite difference methods [34], virtual element methods (VEM) [2,3], weak Galerkin (WG) methods [47], hybrid high order methods [24], generalized barycentric coordinates method (e.g., [18]) and so on. For the Stokes problems, there also exist some recent works. A polygonal finite element was proposed in [43] on convex polygonal partition. Wang and Ye [48] introduced a weak Galerkin method, in which, they used totally discontinuous polynomials on elements and the boundaries, and introduced weak gradient and weak divergence to handle the nonconformity. Cangiani et al. [14] proposed a method using nonconforming virtual elements for each component of the velocity and discontinuous piecewise polynomials for the pressure. Similar method was also presented in [35]. Di Pietro and Lemaire [26] extended the standard Crouzeix–Raviart elements to general meshes. All of these methods are not exactly divergence free and the error estimates for the velocity will thus depend on the pressure. Antonietti et al. [1] introduced a virtual element method based on a 2D stream formulation Stokes problem. Beirão da Veiga et al. [6] proposed a kind of $\boldsymbol{H}^1$ conforming divergence free virtual elements for Stokes problems on 2D polygonal

meshes and generalized it to the 3D polyhedral grids (see also [7,44] for the applications to the Brinkman model and the Navier–Stokes equation).

In this paper, we shall present an exact divergence free elements on polytopal meshes for the Stokes equation formulated as (1). We use discontinuous polynomials to approximate the pressure, and the $\boldsymbol{H}(\mathrm{div})$ virtual elements [4,13] to discretize the velocity. To enforce the tangential continuity, following the idea of WG, we introduce polynomial spaces on the element faces to approximate the tangential trace and define a weak symmetric gradient. We use the stress formulation but not the gradient formulation in order to model more practical model in the engineering applications, and thus the spaces, both of the $\boldsymbol{H}(\mathrm{div})$ conforming virtual element space and the tangential space, should contain rigid body motions to ensure the Korn inequality holds in the discrete level. We note that the proposed velocity element is only $\boldsymbol{H}(\mathrm{div})$ conforming but $\boldsymbol{H}^1$ nonconforming, since the normal continuity of the element is enforced pointwisely while the tangential continuity is only enforced weakly. In this sense, our work can be considered as an extension of MTW element [36] on triangles and XXX elements [49] on tetrahedra to polytopal meshes. It should be also emphasized that developing a divergence free element on 3D is much more difficult, our approach can deal with both 2D and 3D cases.

The tangential spaces only defined on the element boundaries and have no influence on the range of div operator. Due to this property, we obtain an exact divergence free virtual element methods, and the error estimates for the velocity do not depend on the pressure. More precisely, let $(\boldsymbol{u}_h, p_h)$ be the solution of the discrete problem and $(\boldsymbol{u}_I, p_I)$ be the interpolation of the exact solution, we will show that

$$\|\boldsymbol{u}_I - \boldsymbol{u}_h\|_{1,h} + \|p_I - p_h\| \lesssim h^k \|\boldsymbol{u}\|_{k+1} + \nu^{-1} \|h(\boldsymbol{f} - \boldsymbol{\Pi}_h^o \boldsymbol{f})\|,$$

where $\boldsymbol{\Pi}_h^o$ denotes the L^2 projection to piecewise $\boldsymbol{P}_k$ polynomial space.

An outline of the paper is as follows. In Sect. 2 we introduce the weak virtual element spaces. Section 3 concerns with the discrete problem and its well-posedness. The error estimates are given in Sect. 4. In Sect. 5, we report some numerical experiments to verify our results.

Throughout the paper, we use the standard notation for Sobolev spaces and norms. For any region D, $(\cdot,\cdot)_D$ (or $\langle\cdot,\cdot\rangle_D$) denotes the L^2 inner product. The norm and seminorm for the functions in the scalar Sobolev space $H^m(D)$ or the vector Sobolev space $\boldsymbol{H}^m(D)$ ($m \geq 0$) are denoted by $\|\cdot\|_{m,D}$ and $|\cdot|_{m,D}$ respectively. When $m = 0$, we usually omit the subscript and use $\|\cdot\|_D$ to denote the L^2 norm. When D stands for the whole domain Ω, we drop the subscript Ω in the norms and inner products. We also use $\boldsymbol{H}(\mathrm{div})$ ($\boldsymbol{H}(\mathbf{curl})$) to denote the Sobolev space, in which the functions and their divergence ($\mathbf{curl}$) are in $L^2(\boldsymbol{L}^2)$ space.

2 Weak Virtual Element Spaces

Let $\mathcal{T}_h$ be a polytopal mesh of Ω with mesh size h, and $\mathcal{F}_h$ denote the collection of all the $d-1$ dimensional faces. Here we assume that the mesh is shape regular in the sense that: For each element $E \in \mathcal{T}_h$, there exist d real numbers $\gamma_i > 0$ such that, all the constituents (volume, faces, and edges) are star-shaped with respect to a disk of radius $\rho_i > \gamma_i h_E$, where h_E is the diameter of E. With the above geometric conditions, we can establish the trace theorem and inverse inequalities on polytopal elements, see [12,16]. We further assume that the mesh is quasi-uniform in the sense that the diameters of all the elements are of comparable size.

We use $\boldsymbol{n}_E$ to denote the outward unit normal vector defined on ∂E and the subscript will be suppressed if it is clear from the context.

We use P_k to denote the polynomial space of degree $\leq k$, and use $\boldsymbol{P}_k$ for the corresponding vector polynomial space. We usually use bold fonts to indicate vector variables, operators, and spaces throughout this paper.

2.1 $H(\mathbf{div})$-Conforming Virtual Element Spaces

On each element E, following [4] (also [13]), we introduce a local space

$$\boldsymbol{V}_E = \Big\{ \boldsymbol{v} \in \boldsymbol{H}(\mathrm{div}, E) \cap \boldsymbol{H}(\mathbf{curl}, E) : \boldsymbol{v}\cdot\boldsymbol{n} \in P_k(f)\ \forall f \subset \partial E, \\ \mathrm{div}\,\boldsymbol{v} \in P_{k-1}(E),\ \mathbf{curl}\,\boldsymbol{v} \in \mathbf{curl}\,\boldsymbol{P}_k(E) \Big\},$$

We note that the definition is a three dimensional version, while for the two dimension case, the operator $\boldsymbol{H}(\mathbf{curl}, E)$ and $\mathbf{curl}\,\boldsymbol{v} \in \mathbf{curl}\,\boldsymbol{P}_k(E)$ are replaced by $\boldsymbol{H}(\mathrm{rot}, E)$ and $\mathrm{rot}\,\boldsymbol{v} \in P_{k-1}(E)$ respectively. It is obvious that $\boldsymbol{P}_k(E)$ is a subspace of $\boldsymbol{V}_E$, which ensures an optimal approximation property of the space. Unlike the traditional FEMs, there are non-polynomial functions in the space $\boldsymbol{V}_E$, and one does not know explicitly the shape function (a basis) of $\boldsymbol{V}_E$. Thus the element is generally not computable except its degree of freedoms, which is the reason that it is called "virtual element". The novelty of VEM is that only degree of freedom is needed for an accurate discretization. The global virtual element space is

$$\boldsymbol{V}_h^{\mathrm{div}} := \{\boldsymbol{v} \in \boldsymbol{H}(\mathrm{div}, \Omega), \boldsymbol{v}|_E \in \boldsymbol{V}_E\ \forall E \in \mathcal{T}_h, \boldsymbol{v}\cdot\boldsymbol{n} = 0 \text{ on } \partial\Omega\}.$$

It is $\boldsymbol{H}(\mathrm{div}, \Omega)$ conforming as the function is piecewise smooth and the normal component is continuous across the element.

The degree of freedoms (d.o.f.) for functions in $\boldsymbol{V}_E$ are stated as (see Fig. 1 for an illustration of the simplest element in 2D)

$$\text{Type I} \qquad \int_f \boldsymbol{v}\cdot\boldsymbol{n} q_k \,\mathrm{d}s \quad \forall\, q_k \in P_k(f),\ f \subset \partial E,$$

$$\text{Type II} \qquad \int_E \boldsymbol{v}\cdot\boldsymbol{q}_{k-2} \,\mathrm{d}\boldsymbol{x} \quad \forall\, \boldsymbol{q}_{k-2} \in \boldsymbol{G}_{k-2}(E),$$

$$\text{Type III} \qquad \int_E \boldsymbol{v}\cdot\boldsymbol{q}_k \,\mathrm{d}\boldsymbol{x} \quad \forall\, \boldsymbol{q}_k \in \boldsymbol{P}_k(E)\backslash\boldsymbol{G}_k(E),$$

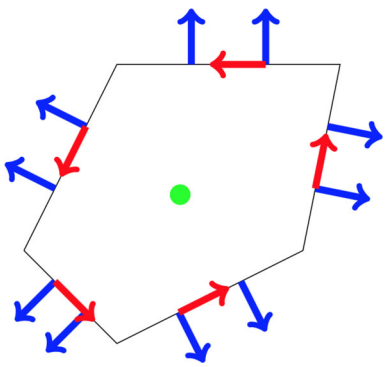

Fig. 1 An illustration of the degree of freedoms of the lowest order element on a polygon. The tangential d.o.f. is colored in red, while the others are for the virtual element space $\boldsymbol{V}_E$ (Color figure online)

where $\boldsymbol{G}_k(E)$ stands for the range of the gradient of the polynomial space $P_{k+1}(E)$. By a direct calculation, the dimension of $\boldsymbol{V}_E$ is

$$\dim(\boldsymbol{V}_E) = \begin{cases} (k+1)n_f + k^2 + k - 1, & \text{if } d = 2, \\ \dfrac{(k+1)(k+2)}{2} n_f + \dfrac{(k+2)(k^2+2k-1)}{2}, & \text{if } d = 3, \end{cases}$$

where n_f denotes the number of $d-1$ dimensional faces of E. The unisolvence can be found in [4], and the 3D case will be discussed briefly below. First of all, the following local problem

$$\operatorname{div} \boldsymbol{v} = \phi, \quad \mathbf{curl}\, \boldsymbol{v} = \boldsymbol{\psi} \text{ in } E, \quad \boldsymbol{v}\cdot\boldsymbol{n} = \varphi \text{ on } \partial E, \tag{2}$$

has a unique solution if and only if the consistent condition $\int_E \phi = \int_{\partial E} \varphi$ holds. We define two local problems: $-\operatorname{div}\operatorname{grad} \Phi = \phi$ in E, $\partial\Phi/\partial\boldsymbol{n} = \varphi$ on ∂E, and $\mathbf{curl}\,\mathbf{curl}\,\Psi = \psi$, $\operatorname{div}\Psi = 0$ in E, $\mathbf{curl}\,\Psi\cdot\boldsymbol{n} = 0$ on ∂E. It is well known that the first problem has a unique solution Φ (up to a constant). The existence and uniqueness of Ψ for the second problem can be found in Corollary 3.1 and Theorem 3.5 in [28]. Setting $\boldsymbol{v} = \nabla\Phi + \mathbf{curl}\,\Psi$ is the desired result.

We now discuss what we can compute using these d.o.f. in the 3D case. Type I d.o.f. will determine piecewise polynomial flux $\boldsymbol{v}\cdot\boldsymbol{n}$ on each face of E. In Type II d.o.f., writing $\boldsymbol{q}_{k-2} = \nabla p_{k-1}$ and using the integration by parts, we have

$$-\int_E \operatorname{div}\boldsymbol{v}\ p_{k-1}\,\mathrm{d}\boldsymbol{x} = \int_E \boldsymbol{v}\cdot\nabla p_{k-1}\,\mathrm{d}\boldsymbol{x} + \int_{\partial E} \boldsymbol{v}\cdot\boldsymbol{n}\ p_{k-1}\,\mathrm{d}s.$$

Therefore $\operatorname{div}\boldsymbol{v} \in P_{k-1}(E)$ can be computed using Type I and Type II d.o.f.. Using the Helmholtz decomposition of $\boldsymbol{P}_k$, the L^2-orthogonal complement of space $\boldsymbol{G}_k(E)$ in $\boldsymbol{P}_k(E)$ is $\mathbf{curl}^*(\mathbf{curl}\,(\boldsymbol{P}_k(E)))$, where $\mathbf{curl}^*$ is the $\boldsymbol{L}^2$-adjoint of $\mathbf{curl}$ and thus Type III is equivalent to

$$\int_E \mathbf{curl}\,\boldsymbol{v}\cdot\boldsymbol{p}_{k-1}\,\mathrm{d}\boldsymbol{x} \quad \forall\ \boldsymbol{p}_{k-1} \in \mathbf{curl}\,(\boldsymbol{P}_k(E)),$$

and consequently $\mathbf{curl}\,\boldsymbol{v} \in \mathbf{curl}\,(\boldsymbol{P}_k(E))$ is uniquely determined by Type III d.o.f.. As $\operatorname{div}\boldsymbol{v}$, $\mathbf{curl}\,\boldsymbol{v}$, $\boldsymbol{v}\cdot\boldsymbol{n}$ are uniquely determined by these d.o.f., the unisolvence then follows from the local problem (2).

On each E, we shall define a $\boldsymbol{L}^2$ projection. For each $\boldsymbol{v} \in \boldsymbol{V}_E$, let $\boldsymbol{\Pi}_E^o\boldsymbol{v} \in \boldsymbol{P}_k(E)$ satisfy

$$\int_E \boldsymbol{\Pi}_E^o\boldsymbol{v}\cdot\boldsymbol{q} := \int_E \boldsymbol{v}\cdot\boldsymbol{q} \quad \forall\, \boldsymbol{q} \in \boldsymbol{P}_k(E).$$

Although the function in $\boldsymbol{V}_E$ is virtual, the $\boldsymbol{L}^2$ projection is computable. In view of Type III d.o.f., we only need to determine $\int_E \boldsymbol{v}\cdot\nabla p_{k+1}$ for $p_{k+1} \in \boldsymbol{P}_{k+1}(E)$ which is again computable through integration by parts

$$\int_E \boldsymbol{v}\cdot\nabla p_{k+1}\,\mathrm{d}\boldsymbol{x} = -\int_E \operatorname{div}\boldsymbol{v}\ p_{k+1}\,\mathrm{d}\boldsymbol{x} + \int_{\partial E} \boldsymbol{v}\cdot\boldsymbol{n}\, p_{k+1}\,\mathrm{d}s.$$

Note that although $p_{k+1} \in P_{k+1}(E)$, the polynomials $\operatorname{div}\boldsymbol{v}$ and $\boldsymbol{v}\cdot\boldsymbol{n}$ have been computed and considered as known.

2.2 Weak Virtual Element Space

In order to approximate the velocity in $\boldsymbol{H}^1$, we also need some d.o.f. on element boundaries to involve the tangential part of the velocity. On one hand, kth-order convergence requires continuity at least with respect to $k-1$ polynomials, see, e.g., [38]. On the other hand, discrete Korn's inequality needs tangential continuity with respect to rigid motion functions on element faces [37]. Thus, on each face $f \in \mathcal{F}_h$, we introduce a space $\boldsymbol{V}_f := \boldsymbol{P}_{k-1}(f) + \mathbf{RM}(f)$, where $\mathbf{RM}(f)$ denotes the space of rigid motions, i.e., $\mathbf{RM}(f) := \{\boldsymbol{c} + R\boldsymbol{x}, \boldsymbol{c} \in \mathbb{R}^{d-1} \text{ and } R \in \mathbb{S}_{d-1}\}$. Here $\mathbb{S}_{d-1}$ is the space of anti-symmetric $(d-1)\times(d-1)$ matrices. The d.o.f. for functions in $\boldsymbol{V}_f$ are

$$\int_f \boldsymbol{v}\cdot\boldsymbol{q}\,\mathrm{d}s \quad \forall \boldsymbol{q} \in \boldsymbol{P}_{k-1}(f) + \mathbf{RM}(f).$$

We note that $\boldsymbol{V}_f = \boldsymbol{P}_{k-1}(f)$ for the case $k > d-2$, and $\boldsymbol{V}_f = \mathbf{RM}(f)$ for the case $k = 1$ in 3D. It is easy to obtain

$$\dim(\boldsymbol{V}_f) = \begin{cases} k, & \text{if } d = 2, \\ k(k+1) + \delta_{k1}, & \text{if } d = 3, \end{cases}$$

where $\delta_{k1} = 1$ for $k = 1$, and $\delta_{k1} = 0$ otherwise. For ease of presentation, we usually express the vector polynomial space $\boldsymbol{V}_f$ in the d dimension, e.g., for all $\boldsymbol{v} \in \boldsymbol{V}_f$, we rewrite it as

$$\boldsymbol{v} = \sum_{i=1}^{d-1} v_i \boldsymbol{\tau}_i, \ v_i = (\boldsymbol{v}\cdot\tau_i) \in P_k(f),$$

where $\boldsymbol{\tau}_i, i = 1, \cdots, d-1$, denote orthogonal unit tangential vectors on the face. Then, the element boundary space is defined as

$$\boldsymbol{V}_h^t := \{\boldsymbol{v}^t, \boldsymbol{v}^t|_f \in \boldsymbol{V}_f, f \in \mathcal{F}_h, \boldsymbol{v}^t = \boldsymbol{0} \text{ on } \partial\Omega\}.$$

Combining the above two kinds of spaces together, gives our weak virtual finite element space:

$$\boldsymbol{V}_h := \left\{\{\boldsymbol{v}_h^{\mathrm{div}}, \boldsymbol{v}_h^t\}, \boldsymbol{v}_h^{\mathrm{div}} \in \boldsymbol{V}_h^{\mathrm{div}}, \boldsymbol{v}_h^t \in \boldsymbol{V}_h^t\right\}.$$

Let N_f and N_E be the number of $d-1$ dimensional faces and elements of $\mathcal{T}_h$. By a explicit computation, the total number of d.o.f. in $\boldsymbol{V}_h$ is

$$\dim(\boldsymbol{V}_h) = \begin{cases} (2k+1)N_f + (k^2+k-1)N_E, & \text{if } d = 2, \\ \left[\dfrac{(k+1)(3k+2)}{2} + \delta_{k1}\right] N_f + \dfrac{(k+2)(k^2+2k-1)}{2} N_E, & \text{if } d = 3. \end{cases}$$

Remark 1 There are two components for the functions $\boldsymbol{v}_h$ in the weak virtual element space $\boldsymbol{V}_h$, that is, the $\boldsymbol{H}(\mathrm{div})$ conforming part $\boldsymbol{v}_h^{\mathrm{div}}$ defined on the whole domain, and tangential part $\boldsymbol{v}_h^t$ associated with element boundaries. For any $\boldsymbol{v}_h = \{\boldsymbol{v}_h^{\mathrm{div}}, \boldsymbol{v}_h^t\}$, the divergence operator can be applied on $\boldsymbol{v}^{\mathrm{div}}$ in the usual sense and further on $\boldsymbol{v}_h$ since $\boldsymbol{v}_h^t$ only defined on a set having a measure of zero in the d dimension. Namely we have $\mathrm{div}\,\boldsymbol{v}_h = \mathrm{div}\,\boldsymbol{v}_h^{\mathrm{div}}$ on Ω.

Remark 2 We note that, compared with MTW element [36] or XXX elements [49] on triangles, our element has more degree of freedoms in the interior of the element. We may reduce some interior d.o.f. using the serendipity technique proposed in [5]. □

With the help of the tangential trace, we can compute a weak symmetric gradient on each element $E \in \mathcal{T}_h$ for functions in $\boldsymbol{V}_h$ following the idea of weak Galerkin method [39,47]. Let $\mathbb{P}^s_{k-1}$ be the space of symmetric matrices, whose components are polynomials of degree at most $k-1$. For any $\boldsymbol{v} = \{\boldsymbol{v}^{\mathrm{div}}, \boldsymbol{v}^t\} \in \boldsymbol{V}_h$, we define $\epsilon^w_E(\boldsymbol{v}) \in \mathbb{P}^s_{k-1}(E)$ satisfying

$$\begin{aligned}(\epsilon^w_E(\boldsymbol{v}), \mathbb{W})_E &:= -(\boldsymbol{v}^{\mathrm{div}}, \operatorname{div}\mathbb{W})_E + \langle \boldsymbol{v}^{\mathrm{div}}\cdot\boldsymbol{n}, (\mathbb{W}\boldsymbol{n})\cdot\boldsymbol{n}\rangle_{\partial E} + \sum_{i=1}^{d-1}\langle \boldsymbol{v}^t\cdot\boldsymbol{\tau}_i, (\mathbb{W}\boldsymbol{n})\cdot\boldsymbol{\tau}_i\rangle_{\partial E}\\ &= -(\Pi^o_E\boldsymbol{v}^{\mathrm{div}}, \operatorname{div}\mathbb{W})_E + \langle \boldsymbol{v}^{\mathrm{div}}\cdot\boldsymbol{n}, (\mathbb{W}\boldsymbol{n})\cdot\boldsymbol{n}\rangle_{\partial E} + \sum_{i=1}^{d-1}\langle \boldsymbol{v}^t\cdot\boldsymbol{\tau}_i, (\mathbb{W}\boldsymbol{n})\cdot\boldsymbol{\tau}_i\rangle_{\partial E}\end{aligned} \tag{3}$$

for all $\mathbb{W} \in \mathbb{P}^s_{k-1}(E)$. Here $(\mathbb{W}\boldsymbol{n})\cdot\boldsymbol{\tau}_i$ denotes the matrix and vector multiplcation $\boldsymbol{n}^{\mathsf{T}}\mathbb{W}\boldsymbol{\tau}_i$. Due to the definition of the d.o.f., all the items in the right hand side are computable.

Remark 3 We can also define the weak symmetric gradient as in [45] by first introducing weak gradient and then taking the symmetric part. All the analysis in this manuscript can be used for this definition.

The triple of polynomials $(\boldsymbol{\Pi}^o_E\boldsymbol{v}^{\mathrm{div}}, \boldsymbol{v}^{\mathrm{div}}\cdot\boldsymbol{n}, \boldsymbol{v}^t)$ can be thought as a special form of the weak function used in the weak Galerkin method. The difference here is the interior polynomial and the flux are connected through a $\boldsymbol{H}(\mathrm{div})$-conforming function $\boldsymbol{v}^{\mathrm{div}}$. Being in $\boldsymbol{H}(\mathrm{div})$, divergence free condition, i.e., $\operatorname{div}\boldsymbol{v}_h = 0$ can be imposed pointwisely. In the definition of our weak virtual element space, $\boldsymbol{v}^t$ is independent of $\boldsymbol{v}^{\mathrm{div}}$. We need to impose the continuity through boundary integrals which are also known as stabilization terms.

2.3 Jumps on the Boundary

If $\boldsymbol{v}^{\mathrm{div}}$ is in $\boldsymbol{H}^1(E)$, recalling the integration by parts

$$(\epsilon(\boldsymbol{v}^{\mathrm{div}}), \mathbb{W})_E = -(\boldsymbol{v}^{\mathrm{div}}, \operatorname{div}\mathbb{W})_E + \langle \boldsymbol{v}^{\mathrm{div}}, \mathbb{W}\boldsymbol{n}\rangle_{\partial E},$$

and using the vector decomposition

$$\boldsymbol{v}^{\mathrm{div}} = (\boldsymbol{v}^{\mathrm{div}}\cdot\boldsymbol{n})\boldsymbol{n} + \sum_{i=1}^{d-1}(\boldsymbol{v}^{\mathrm{div}}\cdot\boldsymbol{\tau}_i)\boldsymbol{\tau}_i, \quad \mathbb{W}\boldsymbol{n} = ((\mathbb{W}\boldsymbol{n})\cdot\boldsymbol{n})\boldsymbol{n} + \sum_{i=1}^{d-1}((\mathbb{W}\boldsymbol{n})\cdot\boldsymbol{\tau}_i)\boldsymbol{\tau}_i,$$

we can rewrite the definition of $\epsilon^w_E(\boldsymbol{v})$ as

$$(\epsilon^w_E(\boldsymbol{v}), \mathbb{W})_E = (\epsilon(\boldsymbol{v}^{\mathrm{div}}), \mathbb{W})_E + \sum_{i=1}^{d-1}\langle(\boldsymbol{v}^t - \boldsymbol{v}^{\mathrm{div}})\cdot\boldsymbol{\tau}_i, (\mathbb{W}\boldsymbol{n})\cdot\boldsymbol{\tau}_i\rangle_{\partial E} \tag{4}$$

which means that $\epsilon^w_E(\boldsymbol{v})$ is the elementwise $\epsilon(\boldsymbol{v}^{\mathrm{div}})$ plus contributions from the boundary. The term $\boldsymbol{v}^{\mathrm{div}}\cdot\boldsymbol{\tau}_i$, however, is not computable, since there is no d.o.f. associated with the tangential trace of an $\boldsymbol{H}(\mathrm{div})$ element.

To get a computable stabilization term, we shall use the second formulation in (3) on the weak symmetric gradient and apply integration by parts to get

$$(\epsilon_E^w(\boldsymbol{v}), \mathbb{W})_E = (\epsilon(\boldsymbol{\Pi}_E^o \boldsymbol{v}), \mathbb{W})_E + \langle \mathcal{J}_{\partial E}^{\boldsymbol{n}}(\boldsymbol{v}), \mathbb{W}\boldsymbol{n}\rangle_{\partial E} + \sum_{i=1}^{d-1} \langle \mathcal{J}_{\partial E}^{\boldsymbol{\tau}_i}(\boldsymbol{v}), \mathbb{W}\boldsymbol{n}\rangle_{\partial E}, \tag{5}$$

where $\mathcal{J}_{\partial E}^{\boldsymbol{n}}(\boldsymbol{v})$ and $\mathcal{J}_{\partial E}^{\boldsymbol{\tau}_i}(\boldsymbol{v})$ denote the differences of $\boldsymbol{v}$ and $\boldsymbol{\Pi}_E^o \boldsymbol{v}$ in the normal and tangential parts respectively, that is

$$\mathcal{J}_{\partial E}^{\boldsymbol{n}}(\boldsymbol{v}) := ((\boldsymbol{v}^{\mathrm{div}} - \boldsymbol{\Pi}_E^o \boldsymbol{v}^{\mathrm{div}})\cdot\boldsymbol{n})\boldsymbol{n}, \quad \mathcal{J}_{\partial E}^{\boldsymbol{\tau}_i}(\boldsymbol{v}) := ((\boldsymbol{v}^t - \boldsymbol{\Pi}_E^o \boldsymbol{v}^{\mathrm{div}})\cdot\boldsymbol{\tau}_i)\boldsymbol{\tau}_i.$$

When the superscript omitted, it indicates the whole jump on the element boundary

$$\mathcal{J}_{\partial E}(\boldsymbol{v}) := \mathcal{J}_{\partial E}^{\boldsymbol{n}}(\boldsymbol{v}) + \mathcal{J}_{\partial E}^{\boldsymbol{\tau}}(\boldsymbol{v}) \quad \text{with} \quad \mathcal{J}_{\partial E}^{\boldsymbol{\tau}}(\boldsymbol{v}) := \sum_{i=1}^{d-1} \mathcal{J}_{\partial E}^{\boldsymbol{\tau}_i}(\boldsymbol{v}).$$

With these notations, we can simply write (5) as

$$(\epsilon_E^w(\boldsymbol{v}), \mathbb{W})_E = (\epsilon(\boldsymbol{\Pi}_E^o \boldsymbol{v}), \mathbb{W})_E + \langle \mathcal{J}_{\partial E}(\boldsymbol{v}), \mathbb{W}\boldsymbol{n}\rangle_{\partial E}.$$

We note the mismatch of the degree of polynomials of $\boldsymbol{v}^t \in \boldsymbol{P}_{k-1}(f)$ and $\boldsymbol{\Pi}_E^o \boldsymbol{v}^{\mathrm{div}} \in \boldsymbol{P}_k(E)$ since to have optimal order of approximation, only the so-called weak continuity of the tangential trace is needed [41]. Therefore we further introduce a projection to the tangential polynomial space on each element face. On the face $f \subset \partial E$, we define $(\boldsymbol{\Pi}_{\partial E}^t \boldsymbol{v})|_f \in \boldsymbol{V}_f$ as

$$\int_f \boldsymbol{\Pi}_{\partial E}^t \boldsymbol{v} \cdot \boldsymbol{q} := \int_f \boldsymbol{v}|_E \cdot \boldsymbol{q} \quad \forall \boldsymbol{q} \in \boldsymbol{V}_f.$$

By the definitions of $\boldsymbol{\Pi}_{\partial E}^t$ and $\boldsymbol{V}_f$, we have

$$\boldsymbol{\Pi}_{\partial E}^t(\boldsymbol{v}\cdot\boldsymbol{\tau}_i\boldsymbol{\tau}_i) = \boldsymbol{\Pi}_{\partial E}^t(\boldsymbol{v})\cdot\boldsymbol{\tau}_i\boldsymbol{\tau}_i, \quad (\boldsymbol{\Pi}_{\partial E}^t \boldsymbol{v})\cdot\boldsymbol{n} = 0.$$

If $\boldsymbol{v}$ is continuous, e.g., $\boldsymbol{v} \in \boldsymbol{H}^1(\Omega)$, we have $(\boldsymbol{\Pi}_{\partial E_1}^t \boldsymbol{v})|_f = (\boldsymbol{\Pi}_{\partial E_2}^t \boldsymbol{v})|_f$, where E_1 and E_2 are the elements having the common face f. The notation $\boldsymbol{\Pi}_{\partial E}$ is defined as

$$\boldsymbol{\Pi}_{\partial E} \boldsymbol{v} := (\boldsymbol{v}\cdot\boldsymbol{n})\boldsymbol{n} + \boldsymbol{\Pi}_{\partial E}^t \boldsymbol{v}.$$

Now, due to $\mathbb{W}\boldsymbol{n} \in \boldsymbol{P}_{k-1}$ on each face, we have the third version of (5)

$$(\epsilon_E^w(\boldsymbol{v}), \mathbb{W})_E = (\epsilon(\boldsymbol{\Pi}_E^o \boldsymbol{v}), \mathbb{W})_E + \langle \boldsymbol{\Pi}_{\partial E} \mathcal{J}_{\partial E}(\boldsymbol{v}), \mathbb{W}\boldsymbol{n}\rangle_{\partial E}. \tag{6}$$

We note that the projection $\boldsymbol{\Pi}_{\partial E}$ acts on the polynomials $\boldsymbol{\Pi}_E^o \boldsymbol{v}^{\mathrm{div}}$ but not the virtual functions $\boldsymbol{v}^{\mathrm{div}}$ and thus the term $\boldsymbol{\Pi}_{\partial E} \mathcal{J}_{\partial E}(\boldsymbol{v})$ is still computable.

Therefore we obtain by the Schwarz inequality, the trace theorem, the inverse inequality, and the assumption of the mesh regularity that

$$\|\epsilon(\boldsymbol{\Pi}_E^o \boldsymbol{v}) - \epsilon_E^w(\boldsymbol{v})\|_E^2 \lesssim h^{-1} \|\boldsymbol{\Pi}_{\partial E} \mathcal{J}_{\partial E}(\boldsymbol{v})\|_{\partial E}^2. \tag{7}$$

2.4 Interpolation Error Analysis

For any $\boldsymbol{v} \in \boldsymbol{H}^1(E)$, $\boldsymbol{I}_E^{\mathrm{div}}\boldsymbol{v} \in \boldsymbol{V}_E$ is defined by the degree of freedoms, i.e.,

$$\int_f \boldsymbol{I}_E^{\mathrm{div}}\boldsymbol{v}\cdot\boldsymbol{n}\, q_k = \int_f \boldsymbol{v}\cdot\boldsymbol{n}\, q_k \quad \forall\, q_k \in P_k(f),\ f \subset \partial E,$$
$$\int_E \boldsymbol{I}_E^{\mathrm{div}}\boldsymbol{v}\cdot\boldsymbol{q}_{k-2} = \int_E \boldsymbol{v}\cdot\boldsymbol{q}_{k-2} \quad \forall\, \boldsymbol{q}_{k-2} \in \boldsymbol{G}_{k-2}(E),$$
$$\int_E \boldsymbol{I}_E^{\mathrm{div}}\boldsymbol{v}\cdot\boldsymbol{q}_k = \int_E \boldsymbol{v}\cdot\boldsymbol{q}_k \quad \forall\, \boldsymbol{q}_k \in \boldsymbol{P}_k(E)\backslash\boldsymbol{G}_k(E).$$

Lemma 1 *We have for any* $\mathbb{W} \in \mathbb{P}^s_{k-1}$ *that*

$$(\epsilon(\boldsymbol{v}), \mathbb{W})_E = (\epsilon_E^w(\boldsymbol{I}_E\boldsymbol{v}), \mathbb{W})_E, \tag{8}$$

where $\boldsymbol{I}_E\boldsymbol{v} := \{\boldsymbol{I}_E^{\mathrm{div}}\boldsymbol{v}, \boldsymbol{\Pi}^t_{\partial E}\boldsymbol{v}\}$.

Proof The identity follows from the definitions of weak symmetric gradient and the interpolation,

$$\begin{aligned}(\epsilon_E^w(\boldsymbol{I}_E\boldsymbol{v}), \mathbb{W})_E &= -(\boldsymbol{I}_E^{\mathrm{div}}\boldsymbol{v}, \mathrm{div}\,\mathbb{W})_E + \langle \boldsymbol{I}_E^{\mathrm{div}}\boldsymbol{v}\cdot\boldsymbol{n}, (\mathbb{W}\boldsymbol{n})\cdot\boldsymbol{n}\rangle_{\partial E} \\ &\quad + \sum_{i=1}^{d-1}\langle \boldsymbol{\Pi}^t_{\partial E}\boldsymbol{v}\cdot\boldsymbol{\tau}_i, (\mathbb{W}\boldsymbol{n})\cdot\boldsymbol{\tau}_i\rangle_{\partial E} \\ &= -(\boldsymbol{v}, \mathrm{div}\,\mathbb{W})_E + \langle \boldsymbol{v}\cdot\boldsymbol{n}, (\mathbb{W}\boldsymbol{n})\cdot\boldsymbol{n}\rangle_{\partial E} + \sum_{i=1}^{d-1}\langle \boldsymbol{v}\cdot\boldsymbol{\tau}_i, (\mathbb{W}\boldsymbol{n})\cdot\boldsymbol{\tau}_i\rangle_{\partial E} \\ &= (\epsilon(\boldsymbol{v}), \mathbb{W})_E.\end{aligned}$$

The proof is completed. □

We then present the following error estimates.

Lemma 2 *Assume that the element* E *is shape regular. Then, for all* $\boldsymbol{v} \in \boldsymbol{H}^{k+1}(E)$, *it is true that*

$$\|\boldsymbol{v} - \boldsymbol{I}_E^{\mathrm{div}}\boldsymbol{v}\|_E + h^{\frac{1}{2}}\|\boldsymbol{v} - \boldsymbol{I}_E^{\mathrm{div}}\boldsymbol{v}\|_{\partial E} \lesssim h^{k+1}\|\boldsymbol{v}\|_{k+1,E}, \tag{9}$$
$$\|\boldsymbol{v} - \boldsymbol{\Pi}_E^o\boldsymbol{v}\|_E + h\|\nabla(\boldsymbol{v} - \boldsymbol{\Pi}_E^o\boldsymbol{v})\|_E + h^{\frac{1}{2}}\|\boldsymbol{v} - \boldsymbol{\Pi}_E^o\boldsymbol{v}\|_{\partial E} \lesssim h^{k+1}\|\boldsymbol{v}\|_{k+1,E}, \tag{10}$$
$$\|\boldsymbol{v} - \boldsymbol{\Pi}_E^o\boldsymbol{I}_E^{\mathrm{div}}\boldsymbol{v}\|_E + h\|\nabla(\boldsymbol{v} - \boldsymbol{\Pi}_E^o\boldsymbol{I}_E^{\mathrm{div}}\boldsymbol{v})\|_E \lesssim h^{k+1}\|\boldsymbol{v}\|_{k+1,E}, \tag{11}$$
$$\|\boldsymbol{\Pi}^t_{\partial E}\mathcal{J}^{\boldsymbol{\tau}}_{\partial E}(\boldsymbol{I}_E\boldsymbol{v})\|_{\partial E} \lesssim h^{k+\frac{1}{2}}\|\boldsymbol{v}\|_{k+1,E}. \tag{12}$$

Proof Since $\boldsymbol{P}_k(E) \subset \boldsymbol{V}_E$, the first three inequalities follow from the standard arguments, see, e.g., [11,12].

For the last inequality, we have

$$\begin{aligned}\|\boldsymbol{\Pi}^t_{\partial E}\mathcal{J}^{\boldsymbol{\tau}}_{\partial E}(\boldsymbol{I}_E\boldsymbol{v})\|^2_{\partial E} &= \sum_{i=1}^{d-1}\|\boldsymbol{\Pi}^t_{\partial E}(\boldsymbol{\Pi}^t_{\partial E}\boldsymbol{v} - \boldsymbol{\Pi}_E^o\boldsymbol{I}_E^{\mathrm{div}}\boldsymbol{v})\cdot\boldsymbol{\tau}_i\boldsymbol{\tau}_i\|^2_{\partial E} \\ &= \sum_{i=1}^{d-1}\|\boldsymbol{\Pi}^t_{\partial E}(\boldsymbol{v} - \boldsymbol{\Pi}_E^o\boldsymbol{I}_E^{\mathrm{div}}\boldsymbol{v})\cdot\boldsymbol{\tau}_i\boldsymbol{\tau}_i\|^2_{\partial E} \\ &\le \|\boldsymbol{v} - \boldsymbol{\Pi}_E^o\boldsymbol{I}_E^{\mathrm{div}}\boldsymbol{v}\|^2_{\partial E},\end{aligned}$$

which, together with the trace theorem and inequality (11), gives the desired result. □

Lemma 3 *On each shape regular element $E \in \mathcal{T}_h$, we have for any $\boldsymbol{u} \in \boldsymbol{H}^{k+1}(E)$ that*

$$\|\epsilon(\boldsymbol{u}) - \epsilon_E^w(\boldsymbol{I}_E\boldsymbol{u})\|_E + h\|\epsilon(\boldsymbol{u}) - \epsilon_E^w(\boldsymbol{I}_E\boldsymbol{u})\|_{1,E} \lesssim h^k\|\boldsymbol{u}\|_{k+1,E}.$$

Proof We note by the triangle inequality that the error can be bounded by two terms

$$\|\epsilon(\boldsymbol{u}) - \epsilon(\boldsymbol{\Pi}_E^o\boldsymbol{I}_E^{\mathrm{div}}\boldsymbol{u})\|_E + h\|\epsilon(\boldsymbol{u}) - \epsilon(\boldsymbol{\Pi}_E^o\boldsymbol{I}_E^{\mathrm{div}}\boldsymbol{u})\|_{1,E}$$

and

$$\|\epsilon(\boldsymbol{\Pi}_E^o\boldsymbol{I}_E^{\mathrm{div}}\boldsymbol{u}) - \epsilon_E^w(\boldsymbol{I}_E\boldsymbol{u})\|_E + h\|\epsilon(\boldsymbol{\Pi}_E^o\boldsymbol{I}_E^{\mathrm{div}}\boldsymbol{u}) - \epsilon_E^w(\boldsymbol{I}_E\boldsymbol{u})\|_{1,E},$$

and the first term can be estimated by Lemma 2. For the second term, we derive from the inverse inequality and inequality (7) that

$$\begin{aligned}
&\|\epsilon(\boldsymbol{\Pi}_E^o\boldsymbol{I}_E^{\mathrm{div}}\boldsymbol{u}) - \epsilon_E^w(\boldsymbol{I}_E\boldsymbol{u})\|_E + h\|\epsilon(\boldsymbol{\Pi}_E^o\boldsymbol{I}_E^{\mathrm{div}}\boldsymbol{u}) - \epsilon_E^w(\boldsymbol{I}_E\boldsymbol{u})\|_{1,E}\\
&\quad\lesssim \|\epsilon(\boldsymbol{\Pi}_E^o\boldsymbol{I}_E^{\mathrm{div}}\boldsymbol{u}) - \epsilon_E^w(\boldsymbol{I}_E\boldsymbol{u})\|_E\\
&\quad\lesssim \|\epsilon(\boldsymbol{\Pi}_E^o\boldsymbol{I}_E^{\mathrm{div}}\boldsymbol{u}) - \epsilon(\boldsymbol{\Pi}_E^o\boldsymbol{u})\|_E + \|\epsilon(\boldsymbol{\Pi}_E^o\boldsymbol{u}) - \epsilon_E^w(\boldsymbol{I}_E\boldsymbol{u})\|_E\\
&\quad\lesssim h^k\|\boldsymbol{u}\|_{k+1,E} + h^{-\frac{1}{2}}\|\boldsymbol{\Pi}_{\partial E}\mathcal{J}_{\partial E}(\boldsymbol{I}_E\boldsymbol{u})\|_{\partial E}.
\end{aligned}$$

Then using the property of the $\boldsymbol{L}^2$ projection, the trace inequality, and again Lemma 2, we have

$$\begin{aligned}
\|\boldsymbol{\Pi}_{\partial E}\mathcal{J}_{\partial E}(\boldsymbol{I}_E\boldsymbol{u})\|_{\partial E} &\le \|\boldsymbol{I}_E^{\mathrm{div}}\boldsymbol{u} - \boldsymbol{\Pi}_E^o\boldsymbol{I}_E^{\mathrm{div}}\boldsymbol{u}\|_{\partial E} + \|\boldsymbol{\Pi}_{\partial E}^t(\boldsymbol{\Pi}_{\partial E}^t\boldsymbol{u} - \boldsymbol{\Pi}_E^o\boldsymbol{I}_E^{\mathrm{div}}\boldsymbol{u})\|_{\partial E}\\
&= \|\boldsymbol{I}_E^{\mathrm{div}}\boldsymbol{u} - \boldsymbol{\Pi}_E^o\boldsymbol{I}_E^{\mathrm{div}}\boldsymbol{u}\|_{\partial E} + \|\boldsymbol{\Pi}_{\partial E}^t(\boldsymbol{u} - \boldsymbol{\Pi}_E^o\boldsymbol{I}_E^{\mathrm{div}}\boldsymbol{u})\|_{\partial E}\\
&\le \|\boldsymbol{I}_E^{\mathrm{div}}\boldsymbol{u} - \boldsymbol{\Pi}_E^o\boldsymbol{I}_E^{\mathrm{div}}\boldsymbol{u}\|_{\partial E} + \|\boldsymbol{u} - \boldsymbol{\Pi}_E^o\boldsymbol{I}_E^{\mathrm{div}}\boldsymbol{u}\|_{\partial E}\\
&\lesssim h^{k+1/2}\|\boldsymbol{u}\|_{k+1,E},
\end{aligned} \tag{13}$$

which yields the desired result. □

When the subscript E is replaced by the mesh size h, the operators introduced above are element-wise defined on the whole domain, i.e., $(\epsilon_h^w(\cdot))|_E = \epsilon_E^w(\cdot)$, $\boldsymbol{\Pi}_h^o|_E = \boldsymbol{\Pi}_E^o$, $\boldsymbol{I}_h^{\mathrm{div}}|_E = \boldsymbol{I}_E^{\mathrm{div}}$, $\boldsymbol{I}_h|_E = \boldsymbol{I}_E$.

3 The Discrete Problem and Its Well-Posedness

In this section we shall present the discretization of Stokes equation (1) using our weak virtual element space. The key is an appropriate stabilization so that the Korn inequality holds on the discrete level.

3.1 Discretization

Let $S_h \subset L_0^2(\Omega)$ be a discontinuous piecewise P_{k-1} element space. Then, the corresponding discrete variational formulation for problem (1) is to seek $\boldsymbol{u}_h = \{\boldsymbol{u}_h^{\mathrm{div}}, \boldsymbol{u}_h^t\} \in \boldsymbol{V}_h$ and $p_h \in S_h$ satisfying

$$\begin{cases} a_h(\boldsymbol{u}_h, \boldsymbol{v}_h) + b(\boldsymbol{v}_h, p_h) = (\boldsymbol{f}, \boldsymbol{\Pi}_h^o\boldsymbol{v}_h^{\mathrm{div}}) & \forall\, \boldsymbol{v}_h \in \boldsymbol{V}_h,\\ b(\boldsymbol{u}_h, q_h) = 0 & \forall\, q_h \in S_h, \end{cases} \tag{14}$$

where

$$a_h(\boldsymbol{u}_h, \boldsymbol{v}_h) := (2\nu\epsilon_h^w(\boldsymbol{u}_h), \epsilon_h^w(\boldsymbol{v}_h)) + 2\nu s_h(\boldsymbol{u}_h, \boldsymbol{v}_h),$$
$$b(\boldsymbol{v}_h, p_h) := -(\operatorname{div} \boldsymbol{v}_h, p_h),$$

with the stabilization term defined as

$$s_h(\boldsymbol{u}_h, \boldsymbol{v}_h) := \sum_{E\in\mathcal{T}_h} \left\langle h^{-1}\boldsymbol{\Pi}_{\partial E}\mathcal{J}_{\partial E}(\boldsymbol{u}_h), \boldsymbol{\Pi}_{\partial E}\mathcal{J}_{\partial E}(\boldsymbol{v}_h)\right\rangle_{\partial E}.$$

We stress that our method is exactly divergence free, since $\operatorname{div} \boldsymbol{V}_h = S_h$.

In the following, we shall discuss the well-posedness of the discrete problem. By the Babuška–Brezzi theory [8], we should define suitable norms on the discrete spaces, and verify the continuity and coercivity of $a_h(\cdot,\cdot)$, and the continuity and the inf-sup condition of $b(\cdot,\cdot)$.

For any $\boldsymbol{v}_h \in \boldsymbol{V}_h$, we introduce a mesh dependent $\boldsymbol{H}^1$ seminorm as

$$\|\boldsymbol{v}_h\|_{1,h}^2 := \sum_{E\in\mathcal{T}_h} \|\boldsymbol{v}_h\|_{1,h,E}^2, \tag{15}$$

where the seminorm on each element is defined as

$$\|\boldsymbol{v}_h\|_{1,h,E}^2 := \|\nabla\boldsymbol{\Pi}_E^o\boldsymbol{v}_h^{\operatorname{div}}\|_E^2 + \|h^{-\frac{1}{2}}\boldsymbol{\Pi}_{\partial E}\mathcal{J}_{\partial E}(\boldsymbol{v}_h)\|_{\partial E}^2.$$

3.2 The Poincaré and Korn Inequalities

In this subsection, we first present some technical lemmas, and then prove the Poincaré and Korn inequalities.

Lemma 4 *On each element $E \in \mathcal{T}_h$, we have for any $\boldsymbol{v} \in \boldsymbol{P}_k(E)$ that*

$$\|\boldsymbol{v} - \boldsymbol{\Pi}_{\partial E}^t\boldsymbol{v}\|_{\partial E} \lesssim h^{\frac{1}{2}}\|\epsilon(\boldsymbol{v})\|_E.$$

Proof By the definition of the space $\boldsymbol{V}_f$, we have for any rigid body motion $\boldsymbol{q} \in \mathbf{RM}(E)$ that

$$(\boldsymbol{\Pi}_{\partial E}^t\boldsymbol{q})|_{\partial E} = \boldsymbol{q}|_{\partial E}.$$

Then, for any $\boldsymbol{q} \in \mathbf{RM}(E)$, it follows from the property of the $\boldsymbol{L}^2$ projection, the trace inequality, and the scaling argument, that

$$\begin{aligned}\|\boldsymbol{v} - \boldsymbol{\Pi}_{\partial E}^t\boldsymbol{v}\|_{\partial E} &= \|(\boldsymbol{v}+\boldsymbol{q}) - \boldsymbol{\Pi}_{\partial E}^t(\boldsymbol{v}+\boldsymbol{q})\|_{\partial E}\\ &\lesssim \|\boldsymbol{v}+\boldsymbol{q}\|_{\partial E}\\ &\lesssim h^{-\frac{1}{2}}\|\boldsymbol{v}+\boldsymbol{q}\|_E + h^{\frac{1}{2}}\|\nabla(\boldsymbol{v}+\boldsymbol{q})\|_E.\end{aligned}$$

On the other hand, for any $\boldsymbol{w} \in \boldsymbol{H}^1(E)$, it holds that

$$\inf_{\boldsymbol{q}\in\mathbf{RM}(E)} \left(h^{-1}\|\boldsymbol{w}+\boldsymbol{q}\|_E + \|\nabla(\boldsymbol{w}+\boldsymbol{q})\|_E\right) \lesssim \|\epsilon(\boldsymbol{w})\|_E.$$

Then the desired inequality follows. □

Lemma 5 *For any $\boldsymbol{v}_h \in \boldsymbol{V}_h^{\operatorname{div}}$, we have*

$$\|\boldsymbol{v}_h - \boldsymbol{\Pi}_E^o\boldsymbol{v}_h\|_E^2 \lesssim h\|\mathcal{J}_{\partial E}^{\boldsymbol{n}}(\boldsymbol{v}_h)\|_{\partial E}^2, \tag{16}$$

and thus by the triangle inequality, we obtain

$$\|\boldsymbol{v}_h\|_E^2 \lesssim \|\boldsymbol{\Pi}_E^o \boldsymbol{v}_h\|_E^2 + h\|\mathcal{J}_{\partial E}^{\boldsymbol{n}}(\boldsymbol{v}_h)\|_{\partial E}^2. \tag{17}$$

Proof We note that $(\boldsymbol{v}_h - \boldsymbol{\Pi}_E^o \boldsymbol{v}_h) \in \boldsymbol{V}_E$. Thus, it can be expressed by the d.o.f.. By the definition of $\boldsymbol{\Pi}_E^o$, all the d.o.f. vanish except $\int_f (\boldsymbol{v}_h - \boldsymbol{\Pi}_E^o \boldsymbol{v}_h)\cdot\boldsymbol{n}$. Using the standard scaling argument and the shape regular assumption, we achieve the inequality (16). □

Lemma 6 *It is true for any* $\boldsymbol{v}_h = \{\boldsymbol{v}_h^{\mathrm{div}}, \boldsymbol{v}_h^t\} \in \boldsymbol{V}_h$ *that*

$$\|\mathcal{J}_{\partial E}(\boldsymbol{v}_h)\|_{\partial E}^2 \lesssim \|\boldsymbol{\Pi}_{\partial E}\mathcal{J}_{\partial E}(\boldsymbol{v}_h)\|_{\partial E}^2 + h\|\epsilon(\boldsymbol{\Pi}_E^o \boldsymbol{v}_h^{\mathrm{div}})\|_E^2 \le h\|\boldsymbol{v}_h\|_{1,h}^2. \tag{18}$$

Proof We only need to estimate the norm of the jump on the tangential directions as the one for the normal jump $\mathcal{J}_{\partial E}^{\boldsymbol{n}}(\boldsymbol{v}_h)$ appears in the right hand side. It follows from the triangle inequality and Lemma 4 that

$$\begin{aligned}
\|\mathcal{J}_{\partial E}^{\boldsymbol{\tau}_i}(\boldsymbol{v}_h)\|_{\partial E}^2 &= \|(\boldsymbol{v}^t - \boldsymbol{\Pi}_E^o \boldsymbol{v}_h^{\mathrm{div}})\cdot\boldsymbol{\tau}_i\|_{\partial E}^2 \\
&\lesssim \|(\boldsymbol{v}^t - \boldsymbol{\Pi}_{\partial E}^t \boldsymbol{\Pi}_E^o \boldsymbol{v}_h^{\mathrm{div}})\cdot\boldsymbol{\tau}_i\|_{\partial E}^2 + \|(\boldsymbol{\Pi}_{\partial E}^t \boldsymbol{\Pi}_E^o \boldsymbol{v}_h^{\mathrm{div}} - \boldsymbol{\Pi}_E^o \boldsymbol{v}_h^{\mathrm{div}})\cdot\boldsymbol{\tau}_i\|_{\partial E}^2 \\
&\lesssim \|\boldsymbol{\Pi}_{\partial E}^t \mathcal{J}_{\partial E}^{\boldsymbol{\tau}_i}(\boldsymbol{v}_h)\|_{\partial E}^2 + h\|\epsilon(\boldsymbol{\Pi}_E^o \boldsymbol{v}_h^{\mathrm{div}})\|_E^2.
\end{aligned}$$

Then summing over the inequality for tangential directions completes the proof. □

As traditionally used in the discontinuous Galerkin methods, the notation $[\cdot]_f$ stands for the jump of functions across the interior face $f \in \mathcal{F}_h$. When f is an outer boundary face, we use the same notation to indicate the function values.

Lemma 7 *For each face* f*, let* $\mathcal{E}_f$ *be the set of the elements taking* f *as a face. Then, for all* $\boldsymbol{v}_h = \{\boldsymbol{v}_h^{\mathrm{div}}, \boldsymbol{v}_h^t\} \in \boldsymbol{V}_h$*, we have*

$$\|[\boldsymbol{\Pi}_h^o \boldsymbol{v}_h^{\mathrm{div}}]\|_f^2 \lesssim \sum_{E\in\mathcal{E}_f} \left(\|\boldsymbol{\Pi}_{\partial E}\mathcal{J}_{\partial E}(\boldsymbol{v}_h)\|_{\partial E}^2 + h\|\epsilon(\boldsymbol{\Pi}_E^o \boldsymbol{v}_h^{\mathrm{div}})\|_E^2\right). \tag{19}$$

Proof We note that the normal component $\boldsymbol{v}_h^{\mathrm{div}}\cdot\boldsymbol{n}$ is continuous across f and $\boldsymbol{v}_h^t$ is a single value on f, and both of them vanish on the outer boundary. Then it follows from the triangle inequality that

$$\|[\boldsymbol{\Pi}_h^o \boldsymbol{v}_h^{\mathrm{div}}]\|_f^2 \lesssim \sum_{E\in\mathcal{E}_f} \|\mathcal{J}_{\partial E}(\boldsymbol{v}_h)\|_{L^2(\partial E)}^2,$$

which, together with Lemma 6, gives the desired result. □

Lemma 8 *For any* $\boldsymbol{v}_h = \{\boldsymbol{v}_h^{\mathrm{div}}, \boldsymbol{v}_h^t\} \in \boldsymbol{V}_h$*, we have the discrete Poincaré inequality:*

$$\|\boldsymbol{v}_h^{\mathrm{div}}\| \lesssim \|\boldsymbol{v}_h\|_{1,h}.$$

Proof Using the general framework of the Poincaré inequality in [9], we have

$$\begin{aligned}
\|\boldsymbol{\Pi}_h^o \boldsymbol{v}_h^{\mathrm{div}}\|^2 &\lesssim \sum_{E\in\mathcal{T}_h} \|\nabla\boldsymbol{\Pi}_h^o \boldsymbol{v}_h^{\mathrm{div}}\|_E^2 + h^{-1}\sum_{f\in\mathcal{F}_h} \left\|\left[\boldsymbol{\Pi}_h^o \boldsymbol{v}_h^{\mathrm{div}}\right]\right\|_f^2 \\
&\lesssim \sum_{E\in\mathcal{T}_h} \left(\|\nabla\boldsymbol{\Pi}_h^o \boldsymbol{v}_h^{\mathrm{div}}\|_E^2 + h^{-1}\|\boldsymbol{\Pi}_{\partial E}\mathcal{J}_{\partial E}(\boldsymbol{v}_h)\|_{\partial E}^2\right),
\end{aligned}$$

where, in the second inequality, we have used Lemma 7. By inequality (17), we then obtain the desired result. □

Lemma 9 *The discrete Korn inequality holds for any* $\boldsymbol{v}_h = \{\boldsymbol{v}_h^{\mathrm{div}}, \boldsymbol{v}_h^t\} \in \boldsymbol{V}_h$ *that*

$$\|\boldsymbol{v}_h\|_{1,h}^2 \lesssim \|\epsilon_h^w(\boldsymbol{v}_h)\|^2 + h^{-1} \sum_{E\in\mathcal{T}_h} \|\boldsymbol{\Pi}_{\partial E}\mathcal{J}_{\partial E}(\boldsymbol{v}_h)\|_{\partial E}^2.$$

Proof It follows from the Korn inequality for the piecewise $\boldsymbol{H}^1$ vector fields [10] (see also [37]) and inequality (19) that

$$\begin{aligned}\sum_{E\in\mathcal{T}_h} \|\nabla \boldsymbol{\Pi}_h^o \boldsymbol{v}_h^{\mathrm{div}}\|_E^2 &\lesssim \sum_{E\in\mathcal{T}_h} \|\epsilon(\boldsymbol{\Pi}_h^o \boldsymbol{v}_h^{\mathrm{div}})\|_E^2 + h^{-1} \sum_{f\in\mathcal{F}_h} \|[\boldsymbol{\Pi}_h^o \boldsymbol{v}_h^{\mathrm{div}}]\|_f^2 \\ &\lesssim \sum_{E\in\mathcal{T}_h} \left(\|\epsilon(\boldsymbol{\Pi}_h^o \boldsymbol{v}_h^{\mathrm{div}})\|_E^2 + h^{-1}\|\boldsymbol{\Pi}_{\partial E}\mathcal{J}_{\partial E}(\boldsymbol{v}_h)\|_{\partial E}^2\right).\end{aligned}$$

Then the proof is completed by using the triangle inequality and inequality (7). □

3.3 The Well-Posedness of the Discrete Problem

In this subsection, we show that the bilinear form $a_h(\cdot,\cdot)$ is continuous and coercive, the bilinear form $b(\cdot,\cdot)$ is continuous and satisfies the inf-sup condition, and thus the problem has a unique solution.

Lemma 10 *For all* $\boldsymbol{u}_h, \boldsymbol{v}_h \in \boldsymbol{V}_h$, *it holds that*

$$\begin{aligned}a_h(\boldsymbol{u}_h, \boldsymbol{v}_h) &\lesssim \nu\|\boldsymbol{u}_h\|_{1,h}\|\boldsymbol{v}_h\|_{1,h}, \\ a_h(\boldsymbol{u}_h, \boldsymbol{u}_h) &\gtrsim \nu\|\boldsymbol{u}_h\|_{1,h}^2.\end{aligned}$$

Proof The two inequalities follows directly from inequality (7), the definition of the norm, and Lemma 9. □

Lemma 11 *For any* $\boldsymbol{v}_h = \{\boldsymbol{v}_h^{\mathrm{div}}, \boldsymbol{v}_h^t\} \in \boldsymbol{V}_h$ *and* $q_h \in S_h$, *it is true that*

$$b(\boldsymbol{v}_h, q_h) \lesssim \|\boldsymbol{v}_h\|_{1,h}\|q_h\|.$$

Proof By integration by parts and the property of the L^2 projection, we have

$$\begin{aligned}\|\operatorname{div}\boldsymbol{v}_h^{\mathrm{div}} - \operatorname{div}\boldsymbol{\Pi}_h^o\boldsymbol{v}_h^{\mathrm{div}}\|_E^2 &= \int_{\partial E} \operatorname{div}(\boldsymbol{v}_h^{\mathrm{div}} - \boldsymbol{\Pi}_h^o\boldsymbol{v}_h^{\mathrm{div}})(\boldsymbol{v}_h^{\mathrm{div}} - \boldsymbol{\Pi}_h^o\boldsymbol{v}_h^{\mathrm{div}})\cdot\boldsymbol{n}\,\mathrm{d}s \\ &\le \|\mathcal{J}_{\partial E}^{\boldsymbol{n}}(\boldsymbol{v}_h)\|_{\partial E}\|\operatorname{div}(\boldsymbol{v}_h^{\mathrm{div}} - \boldsymbol{\Pi}_h^o\boldsymbol{v}_h^{\mathrm{div}})\|_{\partial E},\end{aligned}$$

which, together with the assumption of mesh regularity, yields

$$\|\operatorname{div}\boldsymbol{v}_h^{\mathrm{div}} - \operatorname{div}\boldsymbol{\Pi}_h^o\boldsymbol{v}_h^{\mathrm{div}}\|_E \lesssim h^{-\frac{1}{2}}\|\mathcal{J}_{\partial E}^{\boldsymbol{n}}(\boldsymbol{v}_h)\|_{\partial E} \le \|\boldsymbol{v}_h\|_{1,h}.$$

Then, the desired inequality follows from the Schwarz inequality and the triangle inequality. □

Lemma 12 *For any* $p_h \in S_h$, *there exists a* $\boldsymbol{v}_h = \{\boldsymbol{v}_h^{\mathrm{div}}, \boldsymbol{v}_h^t\} \in \boldsymbol{V}_h$ *such that*

$$\operatorname{div}\boldsymbol{v}_h = p_h \quad \text{and} \quad \|\boldsymbol{v}_h\|_{1,h} \lesssim \|p_h\|.$$

Proof It is well known that for any $p_h \in S_h$, there exists a function $\boldsymbol{v} \in \boldsymbol{H}_0^1(\Omega)$ satisfying

$$\operatorname{div}\boldsymbol{v} = p_h \quad \text{and} \quad \|\boldsymbol{v}\|_1 \lesssim \|p_h\|.$$

We define $\boldsymbol{v}_h = \{\boldsymbol{v}_h^{\mathrm{div}}, \boldsymbol{v}_h^t\}$ as $\boldsymbol{v}_h^{\mathrm{div}}|_E = \boldsymbol{I}_E^{\mathrm{div}}\boldsymbol{v}$, $\boldsymbol{v}_h^t|_{\partial E} = \boldsymbol{\Pi}_{\partial E}^t\boldsymbol{v}$. Then, for any $q \in P_{k-1}(E)$, we have

$$\int_E \mathrm{div}\, \boldsymbol{v}_h^{\mathrm{div}}\, q = -\int_E \boldsymbol{v}_h^{\mathrm{div}}\nabla q + \int_{\partial E} \boldsymbol{v}_h^{\mathrm{div}}\cdot\boldsymbol{n}\, q = -\int_E \boldsymbol{v}\nabla q + \int_{\partial E} \boldsymbol{v}\cdot\boldsymbol{n}\, q = \int_E \mathrm{div}\, \boldsymbol{v}\, q.$$

By noting $\mathrm{div}\, \boldsymbol{v} = p_h \in P_{k-1}$ on E, we obtain the equality

$$\mathrm{div}\, \boldsymbol{v}_h = \mathrm{div}\, \boldsymbol{v}_h^{\mathrm{div}} = p_h.$$

It follows from the triangle inequality, the inverse inequality, and inequalities (10), (11), that

$$\begin{aligned}\|\nabla \boldsymbol{\Pi}_E^o \boldsymbol{v}_h^{\mathrm{div}}\|_E &\le \|\nabla \boldsymbol{v}\|_E + \|\nabla(\boldsymbol{v} - \boldsymbol{\Pi}_E^o\boldsymbol{v})\|_E + \|\nabla(\boldsymbol{\Pi}_E^o\boldsymbol{v} - \boldsymbol{\Pi}_E^o\boldsymbol{v}_h^{\mathrm{div}})\|_E \\ &\lesssim \|\nabla \boldsymbol{v}\|_E + h^{-1}\|\boldsymbol{\Pi}_E^o(\boldsymbol{v} - \boldsymbol{v}_h^{\mathrm{div}})\|_E \lesssim \|\nabla \boldsymbol{v}\|_E.\end{aligned}$$

The inequalities (10) and (12) give

$$\|\boldsymbol{\Pi}_E \mathcal{J}_{\partial E}(\boldsymbol{v}_h)\|_{\partial E}^2 = \|\mathcal{J}_{\partial E}^{\boldsymbol{n}}(\boldsymbol{v}_h)\|_{\partial E}^2 + \|\boldsymbol{\Pi}_{\partial E}^t \mathcal{J}_{\partial E}^{\boldsymbol{\tau}}(\boldsymbol{v}_h)\|_{\partial E}^2 \lesssim h\|\nabla \boldsymbol{v}\|_E.$$

Then the desired result follows. □

From Lemmas 10–12 and the standard framework for saddle point problems [8], we conclude the well-posedness of the discretization.

Theorem 1 *There exists a unique pair of solution* $(\boldsymbol{u}_h, p_h)$ *to problem* (14) *and*

$$\nu\|\boldsymbol{u}_h\|_{1,h} + \|p_h\| \lesssim \|\boldsymbol{\Pi}_h^o \boldsymbol{f}\|. \tag{20}$$

4 Error Analysis

In this section, we assume that $(\boldsymbol{u}, p) \in (\boldsymbol{H}^{k+1} \cap \boldsymbol{H}_0^1) \times (H^k \cap L_0^2)$ is the weak solution of problem (1), and define the interpolation $\boldsymbol{u}_I = \{\boldsymbol{u}_I^{\mathrm{div}}, \boldsymbol{u}_I^t\}$ as $\boldsymbol{u}_I^{\mathrm{div}}|_E = \boldsymbol{I}_E^{\mathrm{div}}\boldsymbol{u}$, $\boldsymbol{u}_I^t|_{\partial E} = \boldsymbol{\Pi}_{\partial E}^t\boldsymbol{u}$, $p_I = Q_h p$, where Q_h denotes the L^2 projection to the space S_h. We shall estimate $\boldsymbol{u}_h - \boldsymbol{u}_I$ and $p_h - p_I$.

4.1 Error Equation

Let $\boldsymbol{v}_h \in \boldsymbol{V}_h$ and $\mathrm{div}\, \boldsymbol{v}_h = 0$. We compute the error equation

$$\begin{aligned}a_h(\boldsymbol{u}_h - \boldsymbol{u}_I, \boldsymbol{v}_h) &= (\boldsymbol{\Pi}_h^o \boldsymbol{f}, \boldsymbol{v}_h^{\mathrm{div}}) - a_h(\boldsymbol{u}_I, \boldsymbol{v}_h) \\ &= (\boldsymbol{\Pi}_h^o \boldsymbol{f} - \boldsymbol{f}, \boldsymbol{v}_h^{\mathrm{div}}) - (2\nu\, \mathrm{div}\, \epsilon(\boldsymbol{u}) - \nabla p, \boldsymbol{v}_h^{\mathrm{div}}) - a_h(\boldsymbol{u}_I, \boldsymbol{v}_h) \\ &= (\boldsymbol{\Pi}_h^o \boldsymbol{f} - \boldsymbol{f}, \boldsymbol{v}_h^{\mathrm{div}} - \boldsymbol{\Pi}_h^o \boldsymbol{v}_h^{\mathrm{div}}) + 2\nu s_h(\boldsymbol{u}_I, \boldsymbol{v}_h) \\ &\quad + 2\nu\left[-(\mathrm{div}\, \epsilon(\boldsymbol{u}), \boldsymbol{v}_h^{\mathrm{div}}) - (\epsilon_h^w(\boldsymbol{u}_I), \epsilon_h^w(\boldsymbol{v}_h))\right],\end{aligned}$$

where we have used the fact $\mathrm{div}\, \boldsymbol{v}_h^{\mathrm{div}} = 0$ to remove the pressure terms.

For any $\boldsymbol{v}_h = \{\boldsymbol{v}_h^{\mathrm{div}}, \boldsymbol{v}_h^t\} \in \boldsymbol{V}_h$, we derive by integration by parts that

$$\begin{aligned}-(\mathrm{div}\, \epsilon(\boldsymbol{u}), \boldsymbol{\Pi}_h^o \boldsymbol{v}_h^{\mathrm{div}}) &= \sum_{E\in\mathcal{T}_h} (\epsilon(\boldsymbol{u}), \epsilon(\boldsymbol{\Pi}_h^o \boldsymbol{v}_h^{\mathrm{div}}))_E - \langle \epsilon(\boldsymbol{u})\boldsymbol{n}, \boldsymbol{\Pi}_h^o \boldsymbol{v}_h^{\mathrm{div}})\rangle_{\partial E} \\ &= \sum_{E\in\mathcal{T}_h} (\epsilon(\boldsymbol{u}), \epsilon(\boldsymbol{\Pi}_h^o \boldsymbol{v}_h^{\mathrm{div}}))_E + \langle \epsilon(\boldsymbol{u})\boldsymbol{n}, \mathcal{J}_{\partial E}(\boldsymbol{v}_h)\rangle_{\partial E},\end{aligned}$$

where, in the second equality, we have used the fact that

$$\sum_{E\in\mathcal{T}_h}\langle\epsilon(\boldsymbol{u})\boldsymbol{n},\boldsymbol{v}_h^{\mathrm{div}}\cdot\boldsymbol{n}\boldsymbol{n}+\boldsymbol{v}_h^t\rangle_{\partial E}=0,$$

since both $\boldsymbol{v}_h^{\mathrm{div}}\cdot\boldsymbol{n}$ and $\boldsymbol{v}_h^t$ are single values on the faces in Ω and vanish on the outer boundary of Ω. On the other hand, it follows from (5) that

$$\begin{aligned}(\epsilon_h^w(\boldsymbol{u}_I),\epsilon_h^w(\boldsymbol{v}_h)) &= \sum_{E\in\mathcal{T}_h}(\epsilon_h^w(\boldsymbol{u}_I),\epsilon(\boldsymbol{\Pi}_h^o\boldsymbol{v}_h^{\mathrm{div}}))_E+(\epsilon_h^w(\boldsymbol{u}_I),\epsilon_h^w(\boldsymbol{v}_h)-\epsilon(\boldsymbol{\Pi}_h^o\boldsymbol{v}_h^{\mathrm{div}}))_E\\ &= \sum_{E\in\mathcal{T}_h}(\epsilon_h^w(\boldsymbol{u}_I),\epsilon(\boldsymbol{\Pi}_h^o\boldsymbol{v}_h^{\mathrm{div}}))_E+\langle\epsilon_h^w(\boldsymbol{u}_I)\boldsymbol{n},\mathcal{J}_{\partial E}(\boldsymbol{v}_h)\rangle_{\partial E}.\end{aligned}$$

Combining the above two equations and Lemma 1 gives

$$\begin{aligned}&-(\mathrm{div}\,\epsilon(\boldsymbol{u}),\boldsymbol{v}_h^{\mathrm{div}})-(\epsilon_h^w(\boldsymbol{u}_I),\epsilon_h^w(\boldsymbol{v}_h))\\ &\quad=(\mathrm{div}\,\epsilon(\boldsymbol{u}),\boldsymbol{\Pi}_h^o\boldsymbol{v}_h^{\mathrm{div}}-\boldsymbol{v}_h^{\mathrm{div}})+\sum_{E\in\mathcal{T}_h}(\epsilon(\boldsymbol{u})-\epsilon_h^w(\boldsymbol{u}_I),\epsilon(\boldsymbol{\Pi}_h^o\boldsymbol{v}_h^{\mathrm{div}}))\\ &\qquad+\sum_{E\in\mathcal{T}_h}\langle(\epsilon(\boldsymbol{u})-\epsilon_h^w(\boldsymbol{u}_I))\boldsymbol{n},\mathcal{J}_{\partial E}(\boldsymbol{v}_h)\rangle_{\partial E}\\ &\quad=\big((I-\boldsymbol{\Pi}_h^o)\,\mathrm{div}\,\epsilon(\boldsymbol{u}),(I-\boldsymbol{\Pi}_h^o)\boldsymbol{v}_h^{\mathrm{div}}\big)+\sum_{E\in\mathcal{T}_h}\langle(\epsilon(\boldsymbol{u})-\epsilon_h^w(\boldsymbol{u}_I))\boldsymbol{n},\mathcal{J}_{\partial E}(\boldsymbol{v}_h)\rangle_{\partial E}.\end{aligned}$$

Therefore we obtain the error equation

$$\begin{aligned}a_h(\boldsymbol{u}_h-\boldsymbol{u}_I,\boldsymbol{v}_h)&=((I-\boldsymbol{\Pi}_h^o)(\boldsymbol{f}+2\nu\,\mathrm{div}\,\epsilon(\boldsymbol{u})),\boldsymbol{\Pi}_h^o\boldsymbol{v}_h^{\mathrm{div}}-\boldsymbol{v}_h^{\mathrm{div}})-2\nu s_h(\boldsymbol{u}_I,\boldsymbol{v}_h)\\ &\quad+\sum_{E\in\mathcal{T}_h}2\nu\langle(\epsilon(\boldsymbol{u})-\epsilon_h^w(\boldsymbol{u}_I))\boldsymbol{n},\mathcal{J}_{\partial E}(\boldsymbol{v}_h)\rangle_{\partial E}\\ &\triangleq \mathrm{I}_1+\mathrm{I}_2+\mathrm{I}_3.\end{aligned}\tag{21}$$

4.2 Error Estimates

Theorem 2 *Let $(\boldsymbol{u},p)\in(\boldsymbol{H}^{k+1}\cap\boldsymbol{H}_0^1)\times(H^k\cap L_0^2)$ and $(\boldsymbol{u}_h,p_h)\in\boldsymbol{V}_h\times S_h$ be the solutions of Eqs. (1) and (14), and $\boldsymbol{f}\in\boldsymbol{L}^2$. It is true that*

$$\|\boldsymbol{u}_I-\boldsymbol{u}_h\|_{1,h}+\|p_I-p_h\|\lesssim h^k\|\boldsymbol{u}\|_{k+1}+\nu^{-1}h\|\boldsymbol{f}-\boldsymbol{\Pi}_h^o\boldsymbol{f}\|.\tag{22}$$

Moreover, we have

$$\|\nabla\boldsymbol{u}-\nabla_h(\boldsymbol{\Pi}_h^o\boldsymbol{u}_h^{\mathrm{div}})\|\lesssim h^k\|\boldsymbol{u}\|_{k+1}+\nu^{-1}h\|\boldsymbol{f}-\boldsymbol{\Pi}_h^o\boldsymbol{f}\|,\tag{23}$$

$$\|p-p_h\|\lesssim h^k(\|\boldsymbol{u}\|_{k+1}+\|p\|_k)+\nu^{-1}h\|\boldsymbol{f}-\boldsymbol{\Pi}_h^o\boldsymbol{f}\|,\tag{24}$$

where ∇_h denotes the element wise gradient.

Proof Setting $\boldsymbol{v}_h=\boldsymbol{u}_h-\boldsymbol{u}_I$ and using the coercivity of $a_h(\cdot,\cdot)$ and Eq. (21) to get

$$\nu\|\boldsymbol{u}_I-\boldsymbol{u}_h\|_{1,h}^2\lesssim a_h(\boldsymbol{u}_h-\boldsymbol{u}_I,\boldsymbol{v}_h)=\mathrm{I}_1+\mathrm{I}_2+\mathrm{I}_3.\tag{25}$$

We bound the three terms in (25) respectively. For the first term, we have from the Schwarz inequality and inequalities (10) and (16) that

$$\begin{aligned}
\mathrm{I}_1 &\le \left(\|\boldsymbol{f}-\boldsymbol{\Pi}_h^o\boldsymbol{f}\|+2\nu\|\operatorname{div}\epsilon(\boldsymbol{u})-\boldsymbol{\Pi}_h^o(\operatorname{div}\epsilon(\boldsymbol{u}))\|\right)\|\boldsymbol{\Pi}_h^o\boldsymbol{v}_h^{\mathrm{div}}-\boldsymbol{v}_h^{\mathrm{div}}\| \\
&\lesssim \left(h\|\boldsymbol{f}-\boldsymbol{\Pi}_h^o\boldsymbol{f}\|+\nu h^k\|\boldsymbol{u}\|_{k+1}\right)\left(\sum_{E\in\mathcal{T}_h}h^{-1}\|\mathcal{J}_{\partial E}^{\boldsymbol{n}}(\boldsymbol{v}_h)\|_{L^2(\partial E)}^2\right)^{\frac{1}{2}} \\
&\le \left(h\|\boldsymbol{f}-\boldsymbol{\Pi}_h^o\boldsymbol{f}\|+\nu h^k\|\boldsymbol{u}\|_{k+1}\right)\|\boldsymbol{v}_h\|_{1,h}.
\end{aligned}$$

For the second term, it follows from the Schwarz inequality and inequality (13) that

$$\begin{aligned}
\mathrm{I}_2 &= -2\nu\sum_{E\in\mathcal{T}_h}h^{-1}\left\langle\boldsymbol{\Pi}_{\partial E}\mathcal{J}_{\partial E}(\boldsymbol{u}_I),\boldsymbol{\Pi}_{\partial E}\mathcal{J}_{\partial E}(\boldsymbol{v}_h)\right\rangle_{\partial E} \\
&\le 2\nu\sum_{E\in\mathcal{T}_h}h^{-1}\|\boldsymbol{\Pi}_{\partial E}\mathcal{J}_{\partial E}(\boldsymbol{u}_I)\|_{\partial E}\|\boldsymbol{\Pi}_{\partial E}\mathcal{J}_{\partial E}(\boldsymbol{v}_h)\|_{\partial E} \\
&\lesssim \nu h^k\|\boldsymbol{u}\|_{k+1}\|\boldsymbol{v}\|_{1,h}.
\end{aligned}$$

For the third term, we derive by the Schwarz inequality, the trace inequality, Lemma (3), and inequality (18) that

$$\begin{aligned}
\mathrm{I}_3 &\le 2\nu\|(\epsilon(\boldsymbol{u})-\epsilon_h^w(\boldsymbol{u}_I))\boldsymbol{n}\|_{\partial E}\|\mathcal{J}_{\partial E}(\boldsymbol{v}_h)\|_{\partial E} \\
&\lesssim \nu h^k\|\boldsymbol{u}\|_{k+1,E}\|\boldsymbol{v}_h\|_{1,h,E}.
\end{aligned}$$

Then, we have proved that

$$\|\boldsymbol{u}_I-\boldsymbol{u}_h\|_{1,h}\lesssim h^k\|\boldsymbol{u}\|_{k+1}+\nu^{-1}h\|\boldsymbol{f}-\boldsymbol{\Pi}_h^o\boldsymbol{f}\|.$$

The velocity error in inequality (23) follows from the triangle inequality, (22), and Lemmas 2 and 10, that is,

$$\begin{aligned}
\|\nabla\boldsymbol{u}-\nabla_h(\boldsymbol{\Pi}_h^o\boldsymbol{u}_h^{\mathrm{div}})\| &\le \|\nabla\boldsymbol{u}-\nabla_h(\boldsymbol{\Pi}_h^o\boldsymbol{u}_I^{\mathrm{div}})\|+\|\boldsymbol{u}_I-\boldsymbol{u}_h\|_{1,h} \\
&\lesssim h^k\|\boldsymbol{u}\|_{k+1}+\nu^{-1}h\|\boldsymbol{f}-\boldsymbol{\Pi}_h^o\boldsymbol{f}\|.
\end{aligned}$$

We next estimate the error for the pressure. It follows from Lemma 12 that there exists a $\boldsymbol{w}_h=\{\boldsymbol{w}_h^{\mathrm{div}},\boldsymbol{w}_h^t\}\in\boldsymbol{W}_h$ such that

$$\operatorname{div}\boldsymbol{w}_h=\operatorname{div}\boldsymbol{w}_h^{\mathrm{div}}=p_I-p_h\quad\text{and}\quad\|\boldsymbol{w}_h\|_{1,h}\lesssim\|p_I-p_h\|.$$

Then, we derive that

$$\begin{aligned}
\|p_I-p_h\|^2 &= (p_I-p_h,\operatorname{div}\boldsymbol{w}_h) \\
&= (p_I,\operatorname{div}\boldsymbol{w}_h)-(p_h,\operatorname{div}\boldsymbol{w}_h) \\
&= (p_I,\operatorname{div}\boldsymbol{w}_h)+(\boldsymbol{f},\boldsymbol{\Pi}_h^o\boldsymbol{w}_h^{\mathrm{div}})-a_h(\boldsymbol{u}_h,\boldsymbol{w}_h) \\
&= (p_I,\operatorname{div}\boldsymbol{w}_h)+(\boldsymbol{f},\boldsymbol{\Pi}_h^o\boldsymbol{w}_h^{\mathrm{div}}-\boldsymbol{w}_h^{\mathrm{div}}) \\
&\quad+(-2\nu\operatorname{div}\epsilon(\boldsymbol{u})+\nabla p,\boldsymbol{w}_h^{\mathrm{div}})-a_h(\boldsymbol{u}_h,\boldsymbol{w}_h) \\
&= (p_I-p,\operatorname{div}\boldsymbol{w}_h)-\left((I-\boldsymbol{\Pi}_h^o)\boldsymbol{f},(I-\boldsymbol{\Pi}_h^o)\boldsymbol{w}_h^{\mathrm{div}}\right) \\
&\quad+(-2\nu\operatorname{div}\epsilon(\boldsymbol{u}),\boldsymbol{w}_h^{\mathrm{div}})-a_h(\boldsymbol{u}_h,\boldsymbol{w}_h).
\end{aligned}$$

By the definition of the L^2 projection, we have

$$(p_I - p, \operatorname{div} \boldsymbol{w}_h^{\mathrm{div}}) = 0,$$

and therefore, we obtain

$$\begin{aligned}\|p_I - p_h\|^2 &= -\left((I - \boldsymbol{\Pi}_h^o)\boldsymbol{f}, (I - \boldsymbol{\Pi}_h^o)\boldsymbol{w}_h^{\mathrm{div}}\right) + (-2\nu \operatorname{div} \epsilon(\boldsymbol{u}), \boldsymbol{w}_h^{\mathrm{div}}) - a_h(\boldsymbol{u}_h, \boldsymbol{w}_h) \\ &= -\left((I - \boldsymbol{\Pi}_h^o)\boldsymbol{f}, (I - \boldsymbol{\Pi}_h^o)\boldsymbol{w}_h^{\mathrm{div}}\right) + (-2\nu \operatorname{div} \epsilon(\boldsymbol{u}), \boldsymbol{w}_h^{\mathrm{div}}) - a_h(\boldsymbol{u}_I, \boldsymbol{w}_h) \\ &\quad + a_h(\boldsymbol{u}_I - \boldsymbol{u}_h, \boldsymbol{w}_h) \\ &\lesssim (h^k \|\boldsymbol{u}\|_{k+1} + \nu^{-1} h \|\boldsymbol{f} - \boldsymbol{\Pi}_h^o \boldsymbol{f}\|) \|\boldsymbol{w}_h\|_{1,h},\end{aligned}$$

which gives

$$\|p_I - p_h\| \lesssim h^k \|\boldsymbol{u}\|_{k+1} + \nu^{-1} h \|\boldsymbol{f} - \boldsymbol{\Pi}_h^o \boldsymbol{f}\|.$$

Thus,

$$\|p - p_h\| \le \|p - p_I\| + \|p_I - p_h\| \lesssim h^k (\|\boldsymbol{u}\|_{k+1} + \|p\|_k) + \nu^{-1} h \|\boldsymbol{f} - \boldsymbol{\Pi}_h^o \boldsymbol{f}\|.$$

The proof is completed. □

Remark 4 From the error estimates, the term $\|h(\boldsymbol{f} - \boldsymbol{\Pi}_h^o \boldsymbol{f})\|$ is usually a higher order term. If we assume that $\boldsymbol{f}$ is piecewise $\boldsymbol{H}^k$ with respect to $\mathcal{T}_h$, we have

$$\|\boldsymbol{u}_I - \boldsymbol{u}_h\|_{1,h} + \|p_I - p_h\| \lesssim h^k \left(\|\boldsymbol{u}\|_{k+1} + \nu^{-1} h \|\boldsymbol{f}\|_{h,k}\right). \tag{26}$$

Here, $\|\boldsymbol{f}\|_{h,k}$ denotes the piecewise $\boldsymbol{H}^k$ norm. □

4.3 L^2 Error Estimates for the Velocity

To derive the $\boldsymbol{L}^2$ error estimates for the velocity, we first define an auxiliary problem

$$\begin{cases} -\operatorname{div}(2\nu\epsilon(\boldsymbol{\psi})) + \nabla\lambda = \boldsymbol{u}_h - \boldsymbol{u}_I & \text{in } \Omega, \\ \operatorname{div} \boldsymbol{\psi} = 0 & \text{in } \Omega, \\ \boldsymbol{\psi} = \boldsymbol{0} & \text{on } \partial\Omega, \end{cases} \tag{27}$$

and assume the solution of the above problem satisfies the $\boldsymbol{H}^2$ regularity:

$$\nu \|\boldsymbol{\psi}\|_2 + \|\lambda\|_1 \lesssim \|\boldsymbol{u}_I - \boldsymbol{u}_h\|. \tag{28}$$

We have the following $\boldsymbol{L}^2$ error estimate.

Theorem 3 *Provided problem (27) has $\boldsymbol{H}^2$ regularity (28), it holds that*

$$\|\boldsymbol{u} - \boldsymbol{u}_h\| \lesssim h^{k+1} \|\boldsymbol{u}\|_{k+1} + \nu^{-1} h^2 \|\boldsymbol{f} - \boldsymbol{\Pi}_h^o \boldsymbol{f}\|.$$

Proof Setting $\boldsymbol{v}_h = \boldsymbol{u}_h - \boldsymbol{u}_I$ and noting $\operatorname{div}(\boldsymbol{u}_h - \boldsymbol{u}_I) = 0$, we have

$$\begin{aligned}\|\boldsymbol{u}_h - \boldsymbol{u}_I\|^2 &= (-\operatorname{div}(2\nu\epsilon(\boldsymbol{\psi})) + \nabla\lambda, \boldsymbol{v}_h^{\mathrm{div}}) \\ &= (-\operatorname{div}(2\nu\epsilon(\boldsymbol{\psi})), \boldsymbol{v}_h^{\mathrm{div}}) - a_h(\boldsymbol{\psi}_I, \boldsymbol{v}_h) + a_h(\boldsymbol{\psi}_I, \boldsymbol{v}_h),\end{aligned} \tag{29}$$

where $\boldsymbol{\psi}_I = \{\boldsymbol{\psi}_I^{\mathrm{div}}, \boldsymbol{\psi}_I^t\}$ is the interpolation of $\boldsymbol{\psi}$ satisfying $\boldsymbol{\psi}_I^{\mathrm{div}}|_E = \boldsymbol{I}_E^{\mathrm{div}} \boldsymbol{\psi}$, $\boldsymbol{\psi}_I^t|_{\partial E} = \boldsymbol{\Pi}_{\partial E}^t \boldsymbol{\psi}$. The first two terms can be estimated as in Theorem 2, that is

$$(-\operatorname{div}(2\nu\epsilon(\boldsymbol{\psi})), \boldsymbol{v}_h^{\mathrm{div}}) - a_h(\boldsymbol{\psi}_I, \boldsymbol{v}_h) \lesssim h\nu \|\boldsymbol{\psi}\|_2 \|\boldsymbol{v}_h\|_{1,h}.$$

From (21) and Lemma 1, we have

$$\begin{aligned} a_h(\boldsymbol{\psi}_I, \boldsymbol{v}_h) &= a_h(\boldsymbol{u}_h - \boldsymbol{u}_I, \boldsymbol{\psi}_I) \\ &= (\boldsymbol{f} + 2\nu \operatorname{div} \epsilon(\boldsymbol{u}), \boldsymbol{\Pi}_h^o \boldsymbol{\psi}_I^{\mathrm{div}} - \boldsymbol{\psi}_I^{\mathrm{div}}) - 2\nu s_h(\boldsymbol{u}_I, \boldsymbol{\psi}_I) \\ &\quad + \sum_{E \in \mathcal{T}_h} 2\nu \langle (\epsilon(\boldsymbol{u}) - \epsilon_h^w(\boldsymbol{u}_I))\boldsymbol{n}, \mathcal{J}_{\partial E}(\boldsymbol{\psi}_I) \rangle_{\partial E}. \end{aligned}$$

Similarly as the proof of Theorem 2 and using inequalities (10)–(11), we have

$$(\boldsymbol{f} + 2\nu \operatorname{div} \epsilon(\boldsymbol{u}), \boldsymbol{\Pi}_h^o \boldsymbol{\psi}_I^{\mathrm{div}} - \boldsymbol{\psi}_I^{\mathrm{div}}) \lesssim (h^2 \|\boldsymbol{f} - \boldsymbol{\Pi}_h^o \boldsymbol{f}\| + h^{k+1} \nu \|\boldsymbol{u}\|_{k+1}) \|\boldsymbol{\psi}\|_2,$$

and

$$s_h(\boldsymbol{u}_I, \boldsymbol{\psi}_I) = \sum_{E \in \mathcal{T}_h} h^{-1} \left\langle \boldsymbol{\Pi}_{\partial E} \mathcal{J}_{\partial E}(\boldsymbol{u}_I), \boldsymbol{\Pi}_{\partial E} \mathcal{J}_{\partial E}(\boldsymbol{\psi}_I) \right\rangle_{\partial E} \lesssim h^{k+1} \|\boldsymbol{u}\|_{k+1} \|\boldsymbol{\psi}\|_2.$$

By noting the fact that $\boldsymbol{\psi}_I^t$ is a single value on each interior face and vanishes on the outer boundary, we have

$$\sum_{E \in \mathcal{T}_h} \langle \epsilon(\boldsymbol{u})\boldsymbol{n}, \mathcal{J}_{\partial E}(\boldsymbol{\psi}_I) \rangle_{\partial E} = \sum_{E \in \mathcal{T}_h} \langle \epsilon(\boldsymbol{u})\boldsymbol{n}, \boldsymbol{\psi} - \boldsymbol{\Pi}_E^o \boldsymbol{\psi}_I^{\mathrm{div}} \rangle_{\partial E}.$$

On the other hand, from the definition of the L^2 projection $\boldsymbol{\Pi}_{\partial E}^t$, we obtain

$$\sum_{E \in \mathcal{T}_h} \langle \epsilon_h^w(\boldsymbol{u}_I)\boldsymbol{n}, \mathcal{J}_{\partial E}(\boldsymbol{\psi}_I) \rangle_{\partial E} = \sum_{E \in \mathcal{T}_h} \langle \epsilon_h^w(\boldsymbol{u}_I)\boldsymbol{n}, \boldsymbol{\psi} - \boldsymbol{\Pi}_E^o \boldsymbol{\psi}_I^{\mathrm{div}} \rangle_{\partial E}.$$

Thus,

$$\begin{aligned} \sum_{E \in \mathcal{T}_h} \langle (\epsilon(\boldsymbol{u}) - \epsilon_h^w(\boldsymbol{u}_I))\boldsymbol{n}, \mathcal{J}_{\partial E}(\boldsymbol{\psi}_I) \rangle_{\partial E} &= \sum_{E \in \mathcal{T}_h} \langle (\epsilon(\boldsymbol{u}) - \epsilon_h^w(\boldsymbol{u}_I))\boldsymbol{n}, \boldsymbol{\psi} - \boldsymbol{\Pi}_E^o \boldsymbol{\psi}_I^{\mathrm{div}} \rangle_{\partial E} \\ &\leq \sum_{E \in \mathcal{T}_h} \|\epsilon(\boldsymbol{u}) - \epsilon_h^w(\boldsymbol{u}_I)\|_{\partial E} \|\boldsymbol{\psi} - \boldsymbol{\Pi}_E^o \boldsymbol{\psi}_I^{\mathrm{div}}\|_{\partial E} \\ &\lesssim h^{k+1} \|\boldsymbol{u}\|_{k+1} \|\boldsymbol{\psi}\|_2, \end{aligned}$$

where we have used Lemmas 3 and 2 in the last inequality.

Using the $\boldsymbol{H}^2$ regularity assumption (28), we have

$$\begin{aligned} \|\boldsymbol{u}_h - \boldsymbol{u}_I\|^2 &\lesssim h\nu \|\boldsymbol{\psi}\|_2 \|\boldsymbol{u}_h - \boldsymbol{u}_I\|_{1,h} + \nu \|\boldsymbol{\psi}\|_2 (h^{k+1} \|\boldsymbol{u}\|_{k+1} + \nu^{-1} h^2 \|\boldsymbol{f} - \boldsymbol{\Pi}_h^o \boldsymbol{f}\|) \\ &\lesssim h \|\boldsymbol{u}_h - \boldsymbol{u}_I\| (\|\boldsymbol{u}_h - \boldsymbol{u}_I\|_{1,h} + h^k \|\boldsymbol{u}\|_{k+1} + \nu^{-1} h \|\boldsymbol{f} - \boldsymbol{\Pi}_h^o \boldsymbol{f}\|), \end{aligned}$$

which, together with Theorem 2, the triangle inequality, and Lemma 2, leads to the desired result. □

5 Numerical Experiments

In this section, we shall present some numerical tests to verify our theoretical conclusions. Denote $\boldsymbol{e_u} := \boldsymbol{u}_I - \boldsymbol{u}_h$, $e_p := Q_h p - p_h$, and $\tilde{e}_p = p - p_h$. We will test the errors $\|\boldsymbol{e_u}\|_{0,h}$, $\|\boldsymbol{e_u}\|_{1,h}$, $\|e_p\|$, and $\|\tilde{e}_p\|$ for the lowest order method ($k = 1$) on different meshes, where the norm $\|\cdot\|_{0,h}$ is defined as

$$\|\boldsymbol{e_u}\|_{0,h}^2 := \sum_{E \in \mathcal{T}_h} \|\boldsymbol{\Pi}_E^o \boldsymbol{e_u}^{\mathrm{div}}\|_E^2 + \|h^{\frac{1}{2}} \boldsymbol{\Pi}_{\partial E} \mathcal{J}_{\partial E}(\boldsymbol{e_u})\|_{\partial E}^2.$$

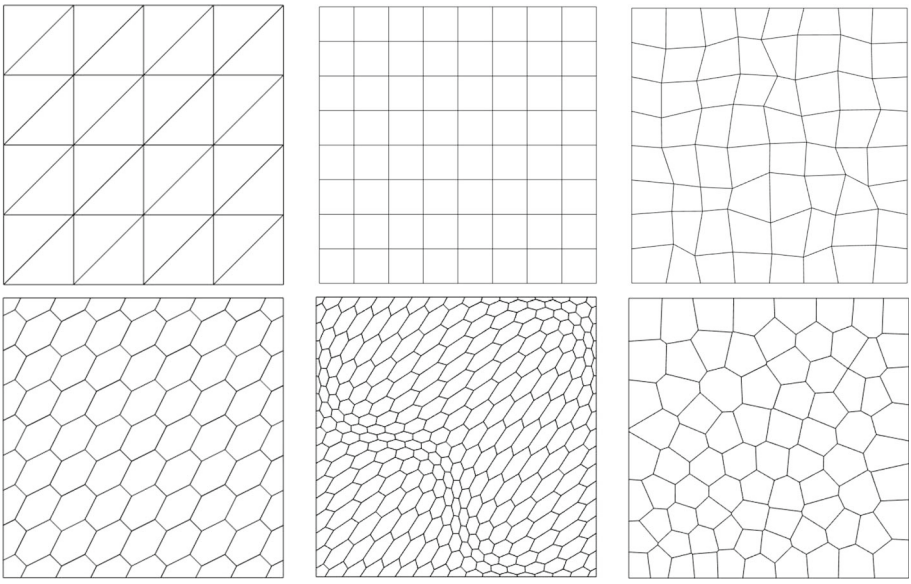

Fig. 2 Illustrations of meshes $\mathcal{T}^1$, $\mathcal{T}^2$, $\mathcal{T}^3$, $\mathcal{T}^4$, $\mathcal{T}^5$, and $\mathcal{T}^6$

We only test the velocity error between the interpolation $\boldsymbol{u}_I$ and solution $\boldsymbol{u}_h$ with respect to the mesh dependent norms $\|\cdot\|_{0,h}$ and $\|\cdot\|_{1,h}$, since the virtual element function is not computable and we cannot measure the error $\boldsymbol{u} - \boldsymbol{u}_h$ directly.

On a two dimensional domain $\Omega = [0, 1]^2$, the velocity and pressure are set to be

$$\begin{aligned} \boldsymbol{u} &= [\sin(x)\sin(y), \cos(x)\cos(y)]^{\mathsf{T}} \\ p &= 2\alpha\left(\cos(x)\sin(y) - \sin(1)(1-\cos(1))\right), \end{aligned}$$

and the corresponding right hand side $\boldsymbol{f} = 2\nu\boldsymbol{u} + 2\alpha[-\sin(x)\sin(y), \cos(x)\cos(y)]^{\mathsf{T}}$. Here α is a constant to be set latter.

We first fixed the parameters $\nu = 1$ and $\alpha = 1$, and tests on six types meshes, that is, uniform triangulation $\mathcal{T}^1$, uniform rectangle mesh $\mathcal{T}^2$, quadrilateral mesh $\mathcal{T}^3$ by perturbing the interior nodes of $\mathcal{T}^2$ with a parameter 0.25 (see [15] for details), polygonal mesh $\mathcal{T}^4$ generated by the dual of the triangle mesh $\mathcal{T}^1$, distorted polygonal mesh $\mathcal{T}^5$, centroidal Voronoi mesh $\mathcal{T}^6$ using two Lloyd's iterations [42], respectively (see Fig. 2 for an illustration).

In Tables 1, 2 and 3, we list the all the resulting errors and the corresponding ratios of the errors on two successive meshes. As expected by Theorems 2–3, it is found that the $\boldsymbol{H}^1$ errors for the velocity and L^2 error for the pressure are of the order $O(h)$ for all types of the meshes, and the $\boldsymbol{L}^2$ error for the velocity is of the order $O(h^2)$ in most cases and a little worse on the perturbed meshes $\mathcal{T}^3$ and distorted polygonal meshes $\mathcal{T}^5$ due to the low mesh quality. On some meshes, we also observe superconvergent phenomenon for the pressure errors (see columns 6–7 in the Tables 1, 2 and 3).

We also do the test on non-convex grids denoted by $\mathcal{T}^7$, see Fig. 3. The errors are listed in Table 4. It is observed the errors $\|\boldsymbol{e}_{\boldsymbol{u}}\|_{0,h}$, $\|\boldsymbol{e}_{\boldsymbol{u}}\|_{1,h}$, and $\|\tilde{e}_p\|$ are optimal. We also have superconvergence for the error $\|e_p\|$.

To clearly see the consequences of pressure-robustness, we next do the tests for different $\alpha = 10^i$, $i = -4, \cdots, 4$ on fixed meshes $\mathcal{T}^1$, $\mathcal{T}^3$, $\mathcal{T}^4$, and $\mathcal{T}^5$ respectively. Although the

Table 1 The errors for a series of the uniform triangle meshes $\mathcal{T}^1$ (upper) and uniform rectangle meshes $\mathcal{T}^2$ (below)

#Dof	$\|e_{\boldsymbol{u}}\|_{0,h}$	r	$\|e_{\boldsymbol{u}}\|_{1,h}$	r	$\|e_p\|$	r	$\|\tilde{e}_p\|$	r
232	1.84e−03	–	3.32e−02	–	4.76418e−02	–	9.42e−02	–
880	4.83e−04	3.81	1.68e−02	1.98	2.46427e−02	1.93	4.76e−02	1.98
3424	1.24e−04	3.89	8.44e−03	1.99	1.23832e−02	1.99	2.38e−02	2.00
13504	3.14e−05	3.96	4.23e−03	1.99	6.19090e−03	2.00	1.19e−02	2.00
53632	7.87e−06	3.99	2.12e−03	2.00	3.09409e−03	2.00	5.96e−03	2.00
560	3.34e−04	–	1.55e−02	–	5.18106e−03	–	5.63e−02	–
2144	8.62e−05	3.87	7.98e−03	1.95	1.70559e−03	3.04	2.81e−02	2.00
8384	2.19e−05	3.94	4.03e−03	1.98	5.17998e−04	3.29	1.40e−02	2.00
33152	5.49e−06	3.98	2.02e−03	1.99	1.49812e−04	3.46	7.01e−03	2.00
131840	1.38e−06	3.99	1.01e−03	2.00	4.20080e−05	3.57	3.50e−03	2.00

Table 2 The errors for a series of quadrilateral meshes $\mathcal{T}^3$ (upper) and polygonal meshes $\mathcal{T}^4$ (below)

#Dof	$\|e_{\boldsymbol{u}}\|_{0,h}$	r	$\|e_{\boldsymbol{u}}\|_{1,h}$	r	$\|e_p\|$	r	$\|\tilde{e}_p\|$	r
560	1.24e−03	–	3.42e−02	–	8.95474e−03	–	5.86e−02	–
2144	3.26e−04	3.81	1.84e−02	1.86	4.73324e−03	1.89	2.95e−02	1.99
8384	8.49e−05	3.83	9.49e−03	1.94	2.47033e−03	1.92	1.49e−02	1.98
33152	2.07e−05	4.10	4.64e−03	2.05	1.19207e−03	2.07	7.42e−03	2.00
131840	5.39e−06	3.84	2.37e−03	1.96	5.90401e−04	2.02	3.71e−03	2.00
978	3.26e−04	–	4.29e−02	–	5.97877e−03	–	5.02e−02	–
3362	9.29e−05	3.51	2.27e−02	1.89	2.25144e−03	2.66	2.57e−02	1.95
12354	2.54e−05	3.66	1.17e−02	1.95	8.25196e−04	2.73	1.30e−02	1.98
47234	6.66e−06	3.81	5.90e−03	1.98	2.96710e−04	2.78	6.54e−03	1.99
184578	1.71e−06	3.90	2.97e−03	1.99	1.05618e−04	2.81	3.28e−03	1.99

Table 3 The errors for a series of the distorted polygonal meshes $\mathcal{T}^5$ (upper) and CVT meshes $\mathcal{T}^6$ (below)

#Dof	$\|e_{\boldsymbol{u}}\|_{0,h}$	r	$\|e_{\boldsymbol{u}}\|_{1,h}$	r	$\|e_p\|$	r	$\|\tilde{e}_p\|$	r
314	1.42e−03	–	7.60e−02	–	1.89704e−02	–	9.52e−02	–
978	6.92e−04	2.05	5.18e−02	1.47	9.88020e−03	1.92	5.33e−02	1.78
3362	2.39e−04	2.90	3.17e−02	1.64	4.19512e−03	2.36	2.87e−02	1.86
12354	6.95e−05	3.43	1.72e−02	1.84	1.55384e−03	2.70	1.48e−02	1.94
47234	1.87e−05	3.71	8.86e−03	1.94	5.50772e−04	2.82	7.47e−03	1.98
217	1.77e−03	–	5.07e−02	–	2.28554e−02	–	1.16e−01	–
841	8.66e−04	2.05	3.88e−02	1.31	1.14238e−02	2.00	5.47e−02	2.12
3391	1.86e−04	4.65	1.95e−02	1.99	4.93532e−03	2.31	2.76e−02	1.98
13660	4.23e−05	4.40	9.64e−03	2.02	2.35466e−03	2.10	1.36e−02	2.03
54553	1.08e−05	3.92	4.87e−03	1.98	1.18903e−03	1.98	6.81e−03	1.99

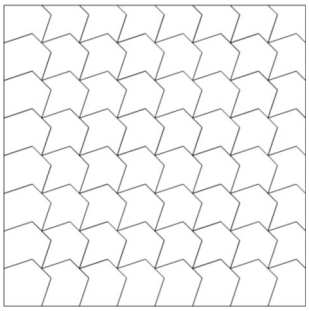

Fig. 3 An illustration of a non-convex mesh $\mathcal{T}^7$

Table 4 The errors for a series of the distorted polygonal meshes $\mathcal{T}^7$

#Dof	$\|e_{\boldsymbol{u}}\|_{0,h}$	r	$\|e_{\boldsymbol{u}}\|_{1,h}$	r	$\|e_p\|$	r	$\|\tilde{e}_p\|$	r
272	2.42e−03	–	9.43e−02	–	1.42047e−02	–	1.16e−01	–
992	6.29e−04	3.84	5.25e−02	1.79	5.95947e−03	2.38	5.78e−02	2.01
3776	1.56e−04	4.04	2.75e−02	1.91	2.30576e−03	2.58	2.87e−02	2.01
14720	3.86e−05	4.03	1.40e−02	1.96	8.55894e−04	2.69	1.43e−02	2.01
58112	9.62e−06	4.01	7.07e−03	1.98	3.10039e−04	2.76	7.15e−03	2.00

Table 5 The L^2 velocity errors $\|e_{\boldsymbol{u}}\|_{0,h}$ with respect to changing pressures

	#Dof	$i=-4$	$i=-2$	$i=-1$	$i=0$	$i=1$	$i=2$	$i=4$
$\mathcal{T}^1$	53632	7.87e−06	7.87e−06	7.87e−06	7.87e−06	7.87e−06	7.88e−06	7.99e−06
$\mathcal{T}^3$	33152	2.13e−05	2.15e−05	2.14e−05	2.09e−05	2.13e−05	2.17e−05	2.30e−05
$\mathcal{T}^4$	47234	6.66e−06	6.66e−06	6.66e−06	6.66e−06	6.66e−06	6.66e−06	7.02e−06
$\mathcal{T}^5$	47234	1.87e−05	1.87e−05	1.87e−05	1.87e−05	1.87e−05	1.87e−05	1.92e−05

Table 6 The H^1 velocity error $\|e_{\boldsymbol{u}}\|_{1,h}$ with respect to changing pressures

	#Dof	$i=-4$	$i=-2$	$i=-1$	$i=0$	$i=1$	$i=2$	$i=4$
$\mathcal{T}^1$	53632	2.12e−03	2.12e−03	2.12e−03	2.12e−03	2.12e−03	2.12e−03	2.21e−03
$\mathcal{T}^3$	33152	4.72e−03	4.70e−03	4.72e−03	4.68e−03	4.68e−03	4.74e−03	4.89e−03
$\mathcal{T}^4$	47234	5.90e−03	5.90e−03	5.90e−03	5.90e−03	5.90e−03	5.90e−03	6.13e−03
$\mathcal{T}^5$	47234	8.86e−03	8.86e−03	8.86e−03	8.86e−03	8.86e−03	8.86e−03	9.16e−03

pressure p varies, the velocity $\boldsymbol{u}$ is unchanged. We list the velocity errors in Tables 5 and 6. On each row, it is observed that both the $\boldsymbol{H}^1$ and $\boldsymbol{L}^2$ errors for the velocity are robust to different pressure scales.

References

1. Antonietti, P.F., Beirão da Veiga, L., Mora, D., Verani, M.: A stream virtual element formulation of the Stokes problem on polygonal meshes. SIAM J. Numer. Anal. **52**(1), 386–404 (2014)

2. Beirão da Veiga, L., Brezzi, F., Cangiani, A., Manzini, G., Marini, L.D., Russo, A.: Basic principles of virtual element methods. Math. Models Methods Appl. Sci. **23**(1), 199–214 (2013)
3. Beirão da Veiga, L., Brezzi, F., Marini, L.D.: Virtual elements for linear elasticity problems. SIAM J. Numer. Anal. **51**(2), 794–812 (2013)
4. Beirão da Veiga, L., Brezzi, F., Marini, L.D., Russo, A.: H(div) and H(curl)-conforming virtual element methods. Numer. Math. **133**(2), 303–332 (2016)
5. Beirão da Veiga, L., Brezzi, F., Marini, L.D., Russo, A.: Serendipity face and edge vem spaces. Rend. Lincei Mat. Appl. **28**(1), 143–181 (2017)
6. Beirão da Veiga, L., Lovadina, C., Vacca, G.: Divergence free virtual elements for the Stokes problem on polygonal meshes. ESAIM Math. Model. Numer. Anal. **51**(2), 509–535 (2017)
7. Beirão da Veiga, L., Lovadina, C., Vacca, G.: Virtual Elements for the Navier-Stokes Problem on Polygonal Meshes. SIAM J. Numer. Anal. **56**(3), 1210–1242 (2018)
8. Boffi, D., Brezzi, F., Fortin, M.: Mixed Finite Element Methods and Applications. Springer, Berlin (2013)
9. Brenner, S.C.: Poincaré-Friedrichs inequalities for piecewise H^1 functions. SIAM J. Numer. Anal. **41**(1), 306–324 (2003)
10. Brenner, S.C.: Korn's inequalities for piecewise H^1 vector fields. Math. Comput. **73**(247), 1067–1087 (2004)
11. Brenner, S.C., Scott, L.R.: The Mathematical Theory of Finite Element Methods, 15th edn. Springer, Berlin (2007)
12. Brenner, S.C., Sung, L.Y.: Virtual element methods on meshes with small edges or faces. Math. Models Methods Appl. Sci. **28**(7), 1291–1336 (2018)
13. Brezzi, F., Falk, R.S., Marini., L.D.: Basic principles of mixed virtual element methods. ESAIM Math. Model. Numer. Anal. **48**, 1227–1240 (2014)
14. Cangiani, A., Gyrya, V., Manzini, G.: The nonconforming virtual element method for the Stokes equations. SIAM J. Numer. Anal. **54**(6), 3411–3435 (2016)
15. Chen, L.: *i*FEM: An Innovative Finite Element Methods Package in MATLAB. Preprint, University of Maryland, College Park (2008)
16. Chen, L., Huang, J.: Some error analysis on virtual element methods. Calcolo **55**(1), 5 (2018)
17. Chen, L., Wang, M., Zhong, L.: Convergence analysis of triangular MAC schemes for two dimensional Stokes equations. J. Sci. Comput. **63**(3), 716–744 (2015)
18. Chen, W., Wang, Y.: Minimal degree H(curl) and H(div) conforming finite elements on polytopal meshes. Math. Comput. **86**(307), 2053–2087 (2017)
19. Cockburn, B., Kanschat, G., Schötzau, D.: A note on discontinuous Galerkin divergence-free solutions of the Navier–Stokes equations. J. Sci. Comput. **31**(1–2), 61–73 (2007)
20. Cockburn, B., Nguyen, N.C., Peraire., J.: A comparison of HDG methods for Stokes flow. J. Sci. Comput. **45**(1–3), 215–237 (2010)
21. Cockburn, B., Sayas, F.-J.: Divergence-conforming HDG methods for Stokes flows. Math. Comput. **83**(288), 1571–1598 (2014)
22. Cockburn, B., Shi, K.: Devising HDG methods for Stokes flow: an overview. Comput. Fluids **98**, 221–229 (2014)
23. De Dios, B.A., Brezzi, F., Marini, L.D., Xu, J., Zikatanov., L.: A simple preconditioner for a discontinuous Galerkin method for the Stokes problem. J. Sci. Comput. **58**(3), 517–547 (2014)
24. Di Pietro, D.A., Ern, A.: A hybrid high-order locking-free method for linear elasticity on general meshes. Comput. Methods Appl. Mech. Eng. **283**, 1–21 (2015)
25. Di Pietro, D.A., Ern, A., Linke, A., Schieweck., F.: A discontinuous skeletal method for the viscosity-dependent Stokes problem. Comput. Methods Appl. Mech. Eng. **306**, 175–195 (2016)
26. Di Pietro, D.A., Lemaire., S.: An extension of the Crouzeix–Raviart space to general meshes with application to quasi-incompressible linear elasticity and Stokes flow. Math. Comput. **84**(291), 1–31 (2015)
27. Falk, R.S., Neilan, M.: Stokes complexes and the construction of stable finite elements with pointwise mass conservation. SIAM J. Numer. Anal. **51**(2), 1308–1326 (2013)
28. Girault, V., Raviart, P.-A.: Finite Element Methods for Navier–Stokes Equations. Springer, Berlin (1986)
29. Guzmán, J., Neilan, M.: Conforming and divergence-free Stokes elements in three dimensions. IMA J. Numer. Anal. **34**(4), 1489–1508 (2014)
30. Guzmán, J., Neilan, M.: Conforming and divergence-free Stokes elements on general triangular meshes. Math. Comput. **83**(285), 15–36 (2014)
31. John, V., Linke, A., Merdon, C., Neilan, M., Rebholz, L.G.: On the divergence constraint in mixed finite element methods for incompressible flows. SIAM Rev. **59**(3), 492–544 (2017)
32. Layton, W.: Introduction to the Numerical Analysis of Incompressible Viscous Flows, vol. 6. SIAM, Tulsa (2008)

33. Lederer, P.L., Linke, A., Merdon, C., Schöberl., J.: Divergence-free reconstruction operators for pressure-robust Stokes discretizations with continuous pressure finite elements. SIAM Rev. **59**(3), 492–544 (2017)
34. Lipnikov, K., Manzini, G., Shashkov, M.: Mimetic finite difference method. J. Comput. Phys. **257**, 1163–1227 (2014)
35. Liu, X., Li, J., Chen, Z.: A nonconforming virtual element method for the Stokes problem on general meshes. Comput. Methods Appl. Mech. Eng. **320**, 694–711 (2017)
36. Mardal, K.A., Tai, X.C., Winther., R.: A robust finite element method for Darcy–Stokes flow. SIAM J. Numer. Anal. **40**(5), 1605–1631 (2002)
37. Mardal, K.A., Winther, R.: An observation on Korn's inequality for nonconforming finite element methods. Math. Comput. **75**(253), 1–6 (2006)
38. Mu, L., Wang, J., Ye, X.: A weak Galerkin finite element method with polynomial reduction. J. Comput. Appl. Math. **285(C)**, 45–58 (2015)
39. Mu, L., Wang, J., Ye, X.: Weak Galerkin finite element methods on polytopal meshes. Int. J. Numer. Anal. Model. **12**(1), 31–53 (2015)
40. Scott, L.R., Vogelius, M.: Norm estimates for a maximal right inverse of the divergence operator in spaces of piecewise polynomials. RAIRO-Modélisation Mathématique et Analyse Numérique **19**(1), 111–143 (1985)
41. Shi, Z., Ming, W.: Finite Element Methods. Science Press, Beijing (2013)
42. Talischi, C., Paulino, G.H., Pereira, A., Menezes, I.F.M.: PolyMesher: a general-purpose mesh generator for polygonal elements written in Matlab. Struct. Multidisc. Optim. **45**, 309–328 (2012)
43. Talischi, C., Pereira, A., Paulino, G.H., Menezes, I.F.M., Carvalho., M.S.: Polygonal finite elements for incompressible fluid flow. Int. J. Numer. Methods Fluids **74**(2), 134–151 (2014)
44. Vacca, G.: An H^1-conforming virtual element for Darcy and Brinkman equations. Math. Models Methods Appl. Sci. **28**(1), 159–194 (2018)
45. Wang, C., Wang, J., Wang, R., Zhang, R.: A locking-free weak Galerkin finite element method for elasticity problems in the primal formulation. J. Comput. Appl. Math. **307**, 346–366 (2016)
46. Wang, J., Ye, X.: New finite element methods in computational fluid dynamics by H(div) elements. SIAM J. Numer. Anal. **45**(3), 1269–1286 (2007)
47. Wang, J., Ye, X.: A weak Galerkin finite element method for second-order elliptic problems. J. Comput. Appl. Math. **241**, 103–115 (2013)
48. Wang, J., Ye, X.: A weak Galerkin finite element method for the Stokes equations. Adv. Comput. Math. **42**(1), 155–174 (2016)
49. Xie, X., Xu, J., Xue, G.: Uniformly-stable finite element methods for Darcy–Stokes–Brinkman models. J. Comput. Math. **26**(3), 437–455 (2008)
50. Zhang, S.: Divergence-free finite elements on tetrahedral grids for $k \geq 6$. Math. Comput. **80**(274), 669–695 (2011)